



TITLE:

# Abstracts of the Papers Published by the Staff Members of the Institute from July, 1973 to June, 1974

AUTHOR(S):

---

CITATION:

Abstracts of the Papers Published by the Staff Members of the Institute from July, 1973 to June, 1974. Bulletin of the Institute for Chemical Research, Kyoto University 1975, 52(5-6): 740-785

ISSUE DATE:

1975-03-31

URL:

<http://hdl.handle.net/2433/76579>

RIGHT:

**Abstracts of the Papers Published by the  
Staff Members of the Institute from  
July, 1973 to June, 1974**

**Nuclear Chemistry**

**Some Properties of Pyrophyllite as a Pressure Medium.** D.-il Lee and H. Mazaki. *Bull. Inst. Chem. Res., Kyoto Univ.*, **51**, 189 (1973).—Characteristics of pyrophyllite used as a pressure medium have been investigated in a pressure range of 0–100 kbar by applying a multianvil high-pressure device. The refractive index of pyrophyllite decreases when the applied pressure increases. This result corresponds to the report by Lees who found the decreased density of pyrophyllite under compression. To understand this superficially unreasonable phenomenon, deformations of the structure were studied by means of electron microscopy. At a pressure of 100 kbar, some of the layered structure of pyrophyllite appear in a massive form which may result in loss of zeolitic water molecules, but no constitutional variation in the layer was found at this pressure.

**Pressure Distribution in a Multianvil High-Pressure Device.** H. Mazaki, D.-il Lee, and S. Shimizu, *J. Phys. E: Scientific Instruments*, **6**, 1072 (1973).—Pressure distribution in an octahedral pressure medium (pyrophyllite) placed in a multianvil (eight-anvil) high-pressure apparatus was measured by applying phase transitions in the calibrated metal (bismuth). It has been shown that the pressure at the edge of the octahedral medium is about 14% lower than that at the center, where the pressure is 25.2 kbar. Confirmation is presented, showing that the distribution is improved when the pressure generated in the medium is increased, and a reasonable uniform pressure distribution is found at the pressure of 77.0 kbar.

**On the Total Probability of K-Electron Shake-Off in Beta-Decay.** Y. Isozumi, T. Mukoyama, and S. Shimizu. *Lett. al Nuovo Cimento*, **10**, 355 (1974).—The rigorous theoretical treatment of the *K*-electron shake-off in beta-decay has been suggested by taking account of the phase space sharing among the three outgoing leptons and the quantum exchange between two continuum electrons. We pointed out a serious mistake in the previous theory of this phenomenon developed by Law and Campbell. We emphasize, in conclusion, that the total *K*-electron shake-off probability per beta-decay calculated by them should be multiplied by a factor of 1/2.

**Internal Excitation and Ionization Accompanying *K* Capture.** T. Mukoyama, Y. Isozumi, T. Kitahara, and S. Shimizu. *Phys. Rev. C*, **8**, 1308 (1973).—The internal excitation and ionization probabilities during *K*-electron capture have

been treated relativistically by the use of hydrogenic wave functions. Relativistic and nonrelativistic calculations for the double  $K$ -hole production probability, the total internal ionization probability, and the energy spectrum of the ejected electrons are presented. The present calculations show that the relativistic effects cause a substantial reduction in the probabilities. The calculated probabilities of the double  $K$ -hole production and the total internal ionization have been compared with the experimental values, and there has been fairly good agreement between the calculated and the recently measured values. The spectral shape of the ejected electrons calculated from the present relativistic theory is similar to that obtained from the previous nonrelativistic and relativistic theories. The theoretical curves are in good agreement with the experimental results in the high-energy region. The discrepancies between the theory and the various experiments are discussed and further work is suggested.

**$L$ -Shell Contribution to Internal Ionization Accompanying Electron Capture.** T. Mukoyama and S. Shimizu. *Phys. Rev. C*, **9**, 2300 (1974).—The  $L$ -shell internal-ionization probability accompanying  $K$  capture,  $K$ -shell internal-ionization probability accompanying  $L$  capture, and the ejected-electron spectrum during these processes have been calculated using screened relativistic hydrogenic wave functions. The screening constant for the daughter atom is determined taking into account the presence of a vacancy resulting from electron capture. The results show that  $L$ -shell contributions are important for the low-energy region of the electron spectrum and for high- $Z$  elements. It is also concluded that the presence of a vacancy in the inner shell of the daughter atom plays an important role.

**$L$ -Shell Internal Ionization Accompanying  $L$  Capture.** T. Mukoyama, T. Kitahara, and S. Shimizu. *Phys. Rev. C*, **9**, 2307 (1974).—The  $L$ -shell internal ionization accompanying  $L$  capture has been considered. Numerical calculations of the internal-ionization probabilities per  $L$  capture and the energy spectra of electrons ejected during this process are presented for low-energy transitions in high- $Z$  elements. Screened relativistic hydrogenic wave functions are used. The effect of the presence of a hole resulting from electron capture is included in the screening constant for the daughter atom. It is shown that the ionization probability per  $L$  capture depends upon  $B_i/E_0$ , where  $E_0$  is the transition energy of the ordinary electron capture and  $B_i$  is the  $L_i$ -shell binding energy of the daughter atom ( $i=1,2,3$ ). The calculated results also predict that observation of this process is possible when the  $K$ -shell internal-ionization process during  $K$  capture is forbidden energetically. Possible experiments to detect this phenomenon are briefly discussed.

**Search for Two-Quantum Annihilation of Positrons in Flight with  $K$ -Shell Electrons.** T. Nagatomo, Y. Nakayama, K. Morimoto, and S. Shimizu. *Phys. Rev. Lett.*, **32**, 1158 (1974).—The two-quantum annihilation of positrons in flight with the  $K$ -shell electrons of silver has been investigated using 300-keV positrons. The experimental result  $(7.7 \pm 6.4) \times 10^{-27} \text{ cm}^2/\text{sr}^2$  has been obtained for the double-differential angular cross section of this process, at 30 and  $-100^\circ$  for each annihila-

tion photon with respect to the incident positron direction.

**External Effects on the Radioactive Half-Life.** S. Shimizu. *Radioisotopes*, **22**, 57 (1973), in Japanese.—Historical review on the study on the external effects, physical, and chemical, on the decay constant  $\lambda$  of some nuclides is presented. In the cases of electron capture and internal conversion the wave function of shell electrons involved at the nucleus may be changed by the chemical bonding and extreme physical effects, high pressure, internal electric field in ferroelectric substances, ultra-high centrifugal field *etc.*, means the change in  $\lambda$  of the radioactive decay or transition. The principle of measuring the minute change in  $\lambda$ , the differential method, using a couple of the radiation detectors is explained. The experimental results with some nuclides obtained to date, including the works with  $^{235}\text{m}\text{U}$  and  $^{99\text{m}}\text{Tc}$  performed by the author's group, are presented and some open problems are also discussed.

**Stopping Powers of Al, Ti, Fe, Cu, Mo, Ag, Sn, Ta, and Au for 7.2 MeV Protons.** R. Ishiwari, N. Shiomi, S. Shirai, and Y. Uemura. *Bull. Inst. Chem. Res., Kyoto Univ.*, **52**, 19 (1974).—Stopping powers of Al, Ti, Fe, Cu, Mo, Ag, Sn, Ta, and Au for 7.2 MeV protons have been measured using a silicon detector. It has been confirmed that the present results for Al, Cu, Ag, and Au are in good agreement with the previous work. It has been found that Nara data are 1.5–3 percent lower than the data of Anderson *et al.* It appears that the deviations are decisive. It has been discussed that Nara data accord with the range data of the compilation of Whaling of Rybakov as well as the stopping power data of Burkig and MacKenzie at 20 MeV in the absolute scale. It has been also shown that Nara data accord well, as a whole, with the tables of Barkas and Berger. Some remarks have been given on Anderson's experiment and Nara experiment. The oscillatory behavior of Bloch constant with increasing  $Z$  has also been discussed.

**Some Experiments on the Radiofrequency System of the Improved Kyoto University Cyclotron.** N. Fujiwara, T. Ohsawa, T. Miyanaga, D. C. Nguyen, K. Fukunaga, and S. Kakigi. *Bull. Inst. Chem. Res., Kyoto Univ.*, **52**, 70 (1974).—Characteristics of the R. F. System of the improved cyclotron are described. The frequency of the R. F. system varies from 10 MHz to 19 MHz by changing the position of the shorting plate inside the resonant line. Frequency trimming is possible with a capacitor and an inductive loop. Two step excitation method is applied to get high dee voltage without suffering from the multipactoring phenomena.

**Improved Kyoto University Cyclotron.** Y. Uemura, K. Fukunaga, S. Kakigi, T. Yanabu, N. Fujiwara, T. Ohsawa, H. Fujita, T. Miyanaga, and D. C. Nguyen. *Bull. Inst. Chem. Res. Kyoto Univ.*, **52**, 87 (1974).—The 105 cm Kyoto University Cyclotron built in 1952 through 1955 had expired its life span and have been remodeled since 1969. All parts of the old cyclotron were replaced with new ones except the main magnet. Efforts were paid to increase the beam intensity, to make the beam energy variable, to accelerate various kinds of ions and to get simple handling and

reliable control. The design principle and the performance characteristics of ion acceleration with the renewed cyclotron are described.

**Residual Radio-Activity of the Kyoto University Cyclotron.** Y. Uemura, T. Nishi, N. Imanishi, and I. Fujiwara. *Bull. Inst. Chem. Res., Kyoto Univ.*, **52**, 124 (1974).—The residual radioactivity of the Kyoto University Cyclotron was surveyed at about one year after its shutdown and before its reconstruction. The radioactive nuclides remained in the electrodes of the cyclotron and in the dust were also assigned.

**Proton Induced Reactions on  $^9\text{Be}$  from 4 to 6 MeV.** M. Yasue, T. Ohsawa, N. Fujiwara, S. Kakigi, D. C. Nguyen, and S. Yamashita. *Bull. Inst. Chem. Res., Kyoto Univ.*, **52**, 177 (1974).—Excitation functions and angular distributions for the  $^9\text{Be}(p, p)^9\text{Be}$ ,  $^9\text{Be}(p, d)^8\text{Be}$ , and  $^9\text{Be}(p, \alpha)^6\text{Li}$  reactions have been measured over the range of proton bombarding energies from 4.0 to 6.0 MeV. In the  $^9\text{Be}(p, p_0)^9\text{Be}(g'nd)$ ,  $^9\text{Be}(p, p_2)^9\text{Be}(2.43)$ , and  $^9\text{Be}(p, \alpha_2)^6\text{Li}(3.56)$  reactions a resonance has been observed at  $E_p=4.7$  MeV, corresponding to the 10.8 MeV state in  $^{10}\text{B}$ . The spin-parity of the 10.8 MeV state in  $^{10}\text{B}$  has been determined to be  $2^+$  by the analysis of the angular distributions for the  $(p, p_2)$  and  $(p, \alpha_2)$  reactions. In the  $^9\text{Be}(p, \alpha_1)^6\text{Li}(2.18)$  and  $^9\text{Be}(p, \alpha_2)^6\text{Li}(3.56)$  reactions, a resonance corresponding to the 11.5 MeV state of  $^{10}\text{Be}$  has been observed at  $E_p=5.5$  MeV.

In the  $^9\text{Be}(p, p_0)^9\text{Be}(g'nd)$  and  $^9\text{Be}(p, \alpha_0)^6\text{Li}(g'nd)$  reactions and in the  $^9\text{Be}(p, p_1)^9\text{Be}(1.67)$  reactions, new resonances have been observed at  $E_p=4.5$  MeV ( $\text{Ex}(^{10}\text{B})=10.6$  MeV) with a width of 200 keV and at  $E_p=5.1$  MeV ( $\text{Ex}(^{10}\text{B})=11.2$  MeV) with a width of 300 keV, respectively. Besides, a gross bump with a width of about 1 MeV has been found in the  $^9\text{Be}(p, p_0)^9\text{Be}(g'nd)$  reaction around  $E_p=4.5$  MeV.

**The  $^7\text{Li}(\alpha, t)\alpha\alpha$  and the  $^6\text{Li}(\alpha, d)\alpha\alpha$  Reaction at 29.4 MeV.** S. Matsuki, S. Yamashita, N. Fujiwara, K. Fukunaga, D. C. Nguyen, and T. Yanabu. *Bull. Inst. Chem. Res., Kyoto Univ.*, **52**, 202 (1974).—Energy spectra of tritons from the  $^7\text{Li}+\alpha$  reaction and of deuterons from the  $^6\text{Li}+\alpha$  reaction were measured from  $6^\circ$  to  $90^\circ$  in the laboratory system. Anomalous broad peaks were observed in the energy spectra at forward angles. They cannot be ascribed to resonances in the residual nucleus  $^8\text{Be}$ . It is suggested that these broad anomalous peaks are due to the sequential decay of the excited state of  $^7\text{Li}$  and that of the excited state of  $^6\text{Li}$ .

Angular distributions of tritons and deuterons from the reactions  $^7\text{Li}(\alpha, t_0)^8\text{Be}_{g'n'd}$ ,  $^7\text{Li}(\alpha, t_1)^8\text{Be}_{1, \text{st}}$ ,  $^6\text{Li}(\alpha, d_0)^8\text{Be}_{g'nd}$ , and  $^6\text{Li}(\alpha, d_1)^8\text{Be}_{1, \text{st}}$  were measured. These angular distributions were confirmed to be dependent on the spin of the residuals as noticed by Siemssen and Dehnhard.

**$^{11}\text{B}(p, \alpha)^8\text{Be}(\alpha)^4\text{He}$  Reaction at 7.3 MeV.** S. Kakigi, N. Fujiwara, K. Fukunaga, T. Ohsawa, D. C. Nguyen, T. Yanabu, M. Yasue, and S. Yamashita. *Bull. Inst. Chem. Res., Kyoto Univ.*, **52**, 218 (1974).—Angular distributions of the first emitted alpha particles and angular correlations between the first and the second

emitted alpha particles were measured. These angular distributions and correlations were analyzed on the basis of the compound nucleus process. The spin of 2 is assigned favorably to the compound nuclear state of  $^{12}\text{C}$  formed in the reaction.

**Energy Dependence of the Reaction  $^9\text{Be}(\text{p}, \text{p}_1)^9\text{Be}^*(1.67)$ .** M. Yasue. *J. Phys. Soc. Japan*, **36**, 1254 (1974).—The  $^9\text{Be}(\text{p}, \text{p}_1)^9\text{Be}^*(1.67)$  reaction is studied in the energy range of protons from 4.2 to 5.5 MeV. Fits of the  $\text{p}_1$  energy spectra to Watson-Migdal's theory show the value of scattering length between a neutron and  $^9\text{Be}$  to be about -20 fm, except at  $E_p=5.1$  MeV, where it is about -30 fm. Analysis with W-M theory shows that the anomaly in the value of the scattering length around  $E_p=5.1$  MeV is due to the overlapping of final state interactions between a proton, a neutron and  $^9\text{Be}$  nucleus.

**Particle Production in Interaction of 8 GeV Protons with Nuclei.** N. Fujiwara, T. Ohsawa, S. Tanaka, and T. Yanabu. *Genshikaku-Kenkyu* **18**, 282 (1973), in Japanese.—An experiment is proposed to clarify the particle production mechanism from nuclei when bombarded by 8 GeV protons of the National Laboratory for High Energy Physics. Particularly, the production of deuterons from light and medium heavy nuclei are noticed to show the short range correlations of two nucleons in the nucleus. The threshold behavior of pion production from the nucleus is also noticed and it is suggested that the popular interpretation of pion production mechanism might be in error.

**Design Studies of Nuclear Instrumentations for the Use of 500 MeV Proton Beam from the Booster Accelerator of National Laboratory for High Energy Physics.** N. Fujiwara, T. Ohsawa and T. Yanabu, and 24 persons of other Institutes and Universities. *Genshikaku-Kenkyu* **18**, 381 (1974), in Japanese.—High energy accelerator now under construction at the National Laboratory for High Energy Physics, Tsukuba, consists of a booster accelerator and a main accelerator. The booster accelerator produces 500 MeV proton pulses at a rating of 20 pulses per second. Among these 20 pulsed beams, 9 pulses of beams are used as injection beams to the main accelerator which produces 8 to 12 GeV protons. Remaining 11 pulses per second can be utilized as a useful tool for the investigation of medium energy nuclear physics and nuclear chemistry. Design studies were performed by tens of physicists and chemists for the construction of nuclear instrumentations necessary to use this 500 MeV proton beam. Design parameters of beam extraction equipments, beam transport systems, radiation detectors, high resolution spectrometers and other chemical treatment apparatus are reported.

## Analytical Chemistry

**Liquid Membrane Electrodes Responsive to Such Organic Anions as Antiseptics and Artificial Sweetenings.** T. Shigematsu, A. Ota, and M. Matsui.

*Bull. Inst. Chem. Res., Kyoto Univ.*, **51**, 268 (1973).—A study was undertaken to evaluate the response and selectivity characteristics of liquid membrane electrodes responsive to organic anions such as antiseptics and artificial sweetenings using the Orion liquid ion-exchange electrode. 1-Decanol solutions of methyltrioctylammonium salts (Kao Quartamine T-08) of organic anions were used as liquid membrane components. The electrodes gave Nernstian responses for the solutions in a concentration range of  $10^{-1}$  to at least  $10^{-3}$  M and were useful at concentrations down to  $10^{-4}$  M. The dissociation constant, pK<sub>a</sub>, obtained from the pH response profile was in good agreement with that in the literature.

**Gas Chromatography of Zinc Pivaloyltrifluoroacetate Adducts with Tri-*n*-Butylphosphate and Tri-*n*-Butylphosphine Oxide.** T. Shigematsu, T. Uchiike, T. Aoki, and M. Matsui. *Bull. Inst. Chem. Res., Kyoto Univ.*, **51**, 273 (1973).—The detection of mixed-ligand complexes of zinc by gas chromatography was reported. Pivaloyltrifluoroacetone was used in combination with organic neutral ligands such as tri-*n*-butylphosphate and tri-*n*-butylphosphine oxide to extract zinc ion synergistically as mixed ligand complexes which were volatile and thermally stable. The composition of the extracted species was considered to be  $\text{Zn}(\text{PTA})_2 \cdot \text{L}$ . Analytical curves were prepared and found usable through a range of 2 to 30  $\mu\text{g}$  zinc.

**The Magnetic Properties of Iron (II) Complexes with 2-(2'-Pyridyl)imidazole and its Derivatives.** Y. Sasaki and T. Shigematsu. *Bull. Chem. Soc. Japan*, **46**, 3438 (1973).—The magnetic susceptibilities and Mössbauer spectra of iron (II) complexes of 2-(2'-pyridyl)imidazole (PI), 2-(6'-methyl-2'-pyridyl)imidazole (6-MPI), and 2-(2'-pyridyl)-benzimidazole (PBI) have been measured in the 4.2–298 K temperature range. The results show that  $\text{Fe}(\text{II})(\text{PI})_3(\text{ClO}_4)_2 \cdot \text{H}_2\text{O}$  and  $\text{Fe}(\text{II})(\text{PBI})_3(\text{ClO}_4)_2 \cdot \text{H}_2\text{O}$  have a spin equilibrium between  $^1\text{A}_1$  and  $^5\text{T}_2$ , while  $\text{Fe}(\text{II})(6\text{-MPI})_3(\text{ClO}_4)_2 \cdot \text{H}_2\text{O}$  does not have such an equilibrium. The temperature dependence and magnitude of the magnetic data for  $\text{Fe}(\text{II})(\text{PBI})_3(\text{ClO}_4)_2 \cdot \text{H}_2\text{O}$  and  $\text{Fe}(\text{II})(6\text{-MPI})_3(\text{ClO}_4)_2 \cdot \text{H}_2\text{O}$  have been calculated by using a parametric ligand-field approximation. The results indicate that the orbital splittings of the  $^5\text{T}_2$  ground state due to trigonal distortion are  $-2000$  and  $-800 \text{ cm}^{-1}$  for  $\text{Fe}(\text{II})(6\text{-MPI})_3(\text{ClO}_4)_2 \cdot \text{H}_2\text{O}$  and  $\text{Fe}(\text{II})(\text{PBI})_3(\text{ClO}_4)_2 \cdot \text{H}_2\text{O}$  respectively.

**The Mössbauer Effect of Several Iron (II) Octahedral Complexes of  $\alpha$ -Dioxime.** Y. Sasaki and T. Shigematsu. *Bull. Chem. Soc. Japan*, **46**, 3590 (1973).—The Mössbauer effect has been used to study the electronic structure of iron porphyrins. The measurement is, however, difficult because of the small quantities of iron present. Therefore, an empirical approach, using simple model compounds, appears to be necessary. Since bis (dimethylglyoximate) diimidazoleiron (II) possesses unsaturated equatorial ligands containing nitrogen donor atoms and biologically-important axial ligands, it is regarded as a model complex of iron porphyrins.

We have studied the electronic structure of iron (II)- $\alpha$ -dioxime complexes contain-

ing pyridine or imidazole as axial ligands by Mössbauer spectroscopy and will report the results here.

**The Preparation and Characterization of Bis [2-(2-pyridyl) imidazole] Iron (II) Complexes.** Y. Sasaki and T. Shigematsu. *Bull. Chem. Soc. Japan*, **47**, 109 (1974).—Bis [2-(2-pyridyl) imidazole] iron (II) complexes,  $\text{Fe}(\text{PI})_2\text{X}_2$  ( $\text{X}=\text{Cl}^-$ ,  $\text{Br}^-$ ,  $\text{NCS}^-$ ,  $\text{N}_3^-$ , and  $\text{CN}^-$ ), were prepared and characterized on the basis of their infrared and Mössbauer spectra and their magnetic data. In  $\text{Fe}(\text{PI})_2(\text{NCS})_2$ , the  $\text{NCS}^-$  groups are N-bonded and are in a *cis* position.  $\text{Fe}(\text{PI})_2(\text{CN})_2\cdot\text{H}_2\text{O}$  also has a *cis* configuration about the  $\text{CN}^-$  ligands. Except for  $\text{Fe}(\text{PI})_2(\text{CN})_2\cdot\text{H}_2\text{O}$ , the magnetic moments of the complexes lie in the 4.94–5.27 B.M. range.  $\text{Fe}(\text{PI})_2(\text{CN})_2\cdot\text{H}_2\text{O}$  is a diamagnetic compound.

**Determination of Cadmium by Atomic Absorption with a Heated Carbon Tube Atomizer; Application to Sea Water.** T. Shigematsu, M. Matsui, and O. Fujino. *Japan Analyst (Bunseki Kagaku)*, **22**, 1162 (1973), in Japanese.—Atomic absorption spectrometry of cadmium was performed by using a carbon tube as an atomizer. The tube was made by boring a carbon rod with a length of 70 mm and with a diameter of 6.35 mm. Smaller bores gave higher sensitivity and a longer life of the tube, but larger bores gave higher reproducibility and lower background.

The peak absorbance of cadmium was dependent on the gas passed through. Among inert gases, helium gave the highest peak absorbance.

A fairly linear calibration curve was obtained in the range of  $(2.5\text{--}15) \times 10^{-11}\text{g}$  of cadmium contained in  $5.0\ \mu\text{l}$  of injection volume; the detection limit was  $3 \times 10^{-12}\text{g}$  and the relative standard variation, 3 per cent. Most cations scarcely interfered with the determination of cadmium even at 1000 times as much as cadmium.

Cadmium content in sea water was determined by extracting it into diisobutyl ketone as DDTC chelate and by using  $20\ \mu\text{l}$  of the organic phase. By this procedure 0.03–1.62 ppb of cadmium were found in the sea water samples.

**Determination of Hydrogen Peroxide by Chemiluminescence.** S. Gohda, Y. Yamashita, Y. Nishikawa, and T. Shigematsu. *Japan Analyst (Bunseki Kagaku)*, **22**, 1180 (1973), in Japanese.—The reaction between hydrogen peroxide and luminol in alkaline aqueous medium was catalyzed by tetrammine-diaquacobalt (III) ions. The chemiluminescence reaction in luminol-cobalt (III)-hydrogen peroxide system ( $8.57 \times 10^{-5}\text{ M}$  luminol,  $0.57\text{ M}$   $\text{Na}_2\text{CO}_3$ ,  $\lesssim 8.57\text{ M}$   $\text{H}_2\text{O}_2$ ,  $1.71 \times 10^{-4}\text{ M}$   $[\text{Co}(\text{H}_2\text{O})_2(\text{NH}_3)_4]^{3+}$ , emission maximum 430 nm) was used for the determination of micro amounts of hydrogen peroxide, and the method was applied to the determination of hydrogen peroxide formed in  $\gamma$ -irradiated water. This system may be used as a dosimeter in the range of  $10^4\text{--}10^7$  roentgen with  $^{60}\text{Co}$   $\gamma$ -rays.

**Coprecipitation of Cobaltous Ion with Calcium Oxalate.** T. Shigematsu, O. Fujino, and M. Matsui. *Radioisotopes*, **22**, 28 (1973).—The coprecipitation behavior of cobaltous ion with calcium oxalate was investigated in a homogeneous precipita-



tion system using dimethyl oxalate. The apparent distribution coefficient of cobaltous ion was considerably affected by the pH values and the acetate concentration, but was not affected by the concentration of cobaltous ion. There was observed much resemblance in behavior between the apparent coefficient obtained from the coprecipitation experiment and the theoretical apparent coefficient which was calculated from the solubility products of calcium and cobalt oxalates and from the stability constants of calcium and cobalt acetates. The true distribution coefficient of cobaltous ion to calcium oxalate had the value of around 0.10 from the coprecipitation experiment at 75°C and the value of 0.14 by the calculation of the solubility product at 25°C.

**Determination of Lead by Atomic Absorption Spectrometry with a Carbon Tube Atomizer.** T. Shigematsu, M. Matsui, O. Fujino, and K. Kinoshita. *Nippon Kagaku Kaishi*, **8**, 2123 (1973), in Japanese.—Atomic absorption spectrometry of lead was studied by using a carbon tube flameless atomizer. The variables affecting sensitivity and reproducibility such as the inside diameter of the tube, the inert gas and its flow rate, and sample injection volume, as well as interference of diverse ions were investigated.

A fairly linear calibration curve was obtained in the range of  $(5\sim 50)H10^{-10}g$  of lead with injection volume of  $5\mu l$ . The detection limit was  $6.5\times 10^{-11}g$  and the relative standard deviation, 2.8 per cent. Most cations, at 100 times as much as lead, scarcely interfered in the determination of lead, but several cations at 1000 times, seriously interfered. Lead content in sea water was determined by extracting it into diisobutyl ketone as diethyl-dithiocarbamate, injecting  $10\mu l$  of the organic phase and measuring the peak absorbance at the wave length of 283.3 nm. With this method, 1.7–8.0 ppb of lead were found in the sea water samples.

**Atomic Absorption Spectrometric Determination of Trace Amounts of Cadmium.** T. Shigematsu. *Bunseki Kiki*, **11**, 530 (1973), in Japanese.—Atomic absorption spectrometry of cadmium was studied by using a carbon tube atomizer. Its application to the analysis of natural waters is presented.

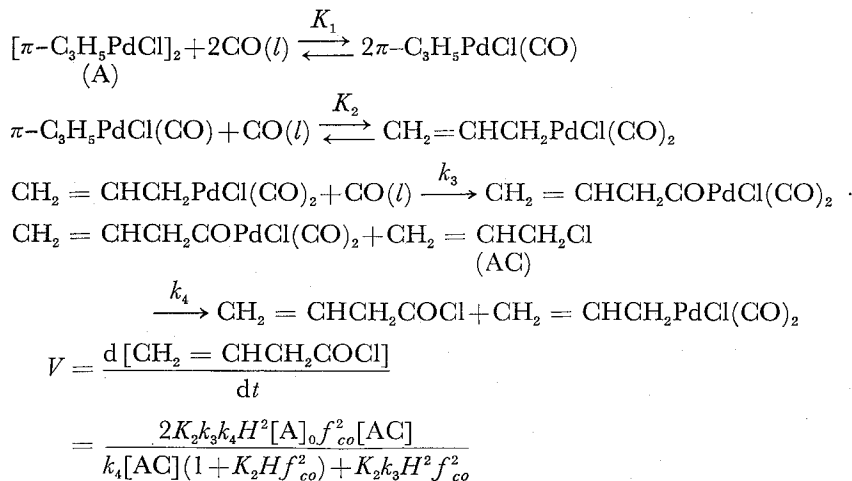
**Chemiluminescence Method for the Determination of Hydrogen Peroxide.** T. Shigematsu. *Bunseki Kiki*, **12**, 36 (1974), in Japanese.—Analytical application of chemiluminescence was reviewed, and the chemiluminescence reaction of cobalt catalysed luminol- $H_2O$  system was illustrated.

## Physical Chemistry

**Kinetics on Palladium Catalyzed Carbonylation of Allyl Chloride under Carbon Monoxide Pressure.** H. Yoshida, N. Sugita, K. Kudo, and Y. Takezaki. *Nippon Kagaku Kaishi*, 1002 (1974), in Japanese.—Synthesis of but-3-enoyl chloride from allyl chloride and carbon monoxide under various pressure in a benzene solution

has been studied kinetically in the presence of a catalytic amount of  $[\pi\text{-C}_3\text{H}_5\text{PdCl}]_2$ .

Based on the assumption of the reaction mechanism proposed in the previous reports by other authors, the rate equation has been derived as shown below:



H; Henry constant of CO,  $f_{\text{CO}}$ ; Fugacity of CO.

Which is in reasonable agreement with the experimental results.

The equilibrium constants, rate constants, Henry constant at 100°C and the over all activation energy have been determined to be  $K_1=23$ ,  $K_2=0.13 \text{ mol}^{-1}\cdot l$ ,  $k_3=1.6 \times 10^2 \text{ mol}^{-1}\cdot l\cdot \text{min}^{-1}$ ,  $k_4=4.2 \text{ mol}^{-1}\cdot l\cdot \text{min}^{-1}$ ,  $H=2.60 \times 10^{-3} \text{ mol}\cdot l^{-1}\cdot \text{atm}^{-1}$  and  $E_a=10.8 \text{ kcal}\cdot \text{mol}^{-1}$ , respectively.

**Cartesian Displacements of Normal Vibrations of 1, 2, 4, 5-Tetracyanobenzene and 1, 2, 4, 5-Tetracyanobenzene- $d_2$  Molecules.** J. Umemura and T. Takenaka. *Bull. Inst. Chem. Res., Kyoto Univ.*, **51**, 206 (1973).—Displacements of the intramolecular normal vibrations of the TCNB and TCNB- $d_2$  molecules were calculated in terms of the Cartesian coordinates, and graphically represented in a diagram. The results were compared with the numerical representation of the normal vibrations by means of the potential energy distribution.

**The Adsorption of Ethylene Glycols and their Cyclic Compounds at the Mercury-Aqueous Solution Interface.** M. Matsumoto, Y. Sakamori, K. Nishizawa, and A. Watanabe. *Colloid and Polymer Science*, **252**, 478 (1974).—Differential double layer capacities were measured at the interface between mercury and aqueous solutions containing ethylene glycols and their cyclic compounds, and free energies of adsorption were calculated in order to study the structure of adsorbed layer of these compounds. Free energies for cyclic compounds were higher than those of others, more than half of the free energies of cyclic compounds being the contribution of the benzene ring. The calculation of adsorbed amounts showed that cyclic compounds were in parallel, and others in inclined orientation on the mercury surface. It was concluded that the adsorption of cyclic compounds was governed by the interaction

between intra-molecular  $\pi$ -electrons and electrons of mercury surface. Free energies of adsorption per  $-\text{CH}_2-$  and  $-\text{OH}$  were calculated to be  $-400$  to  $-600$  kcal/mole, respectively.

**Disappearances of COOH Infrared Bands of Benzoic Acid.** S. Hayashi and J. Umemura. *J. Chem. Phys.*, **60**, 2630 (1974).—Infrared spectra of benzoic acids and benzoic acid-*d* were obtained in the range of temperatures from liquid nitrogen to liquid helium. The  $\text{C}=\text{O}$  stretching band at  $1688\text{ cm}^{-1}$ , the strongest absorption band of this compound in the over-all infrared region at room temperature, decreased in intensity with decreasing temperature and disappears near liquid-helium temperatures. Near this temperature, also lost was the band at  $959\text{ cm}^{-1}$  which has been assigned to the OH out-of-plane vibration. For the deuterated species both bands at  $1689$  and  $1679\text{ cm}^{-1}$ , which have been interpreted as splitting due to Fermi resonance of the  $\text{C}=\text{O}$  stretching vibration, were lost. Close to the positions of these lost bands, alternative bands, which are assignable to the same modes and increase in intensity with decreasing temperature, are found. The results support the postulate proposed in our earlier work that two distinct equilibrium configurations of benzoic acid dimer coexist in the crystal.

**Infrared Attenuated Total Reflection Spectra of Adsorbed Layers at the Interface between a Germanium Electrode and an Aqueous Solution of Sodium Laurate.** T. Higashiyama and T. Takenaka. *J. Phys. Chem.*, **78**, 941 (1974).—Polarized infrared attenuated total reflection (ATR) measurements have been made on thin layers adsorbed on a germanium ATR plate electrode from an aqueous solution of sodium laurate. A platinum plate was immersed in the solution as an auxiliary electrode and was electrically connected to the germanium plate. When necessary, electric potentials lower than  $0.5\text{ V}$  were applied between the two plates. It is found that when the concentration of the aqueous solution is less than *ca.*  $10\text{ mM}$ , the adsorbed layers consist of an assembly of crystallites of lauric acid. The crystallites are monoclinic and uniaxially oriented so that their crystallographic *c* axes make an angle of  $39^\circ$  with the *z* axis normal to the germanium surface.

Reference to the crystal structure of lauric acid indicates that the axes of the hydrocarbon chains of the lauric acid molecules also give rise to uniaxial orientation and make an angle of  $35^\circ$  with the *z* axis. When the concentration of the aqueous solution approaches or exceeds the critical micelle concentration, laurate ion micelles are adsorbed, in which the hydrocarbon chains are flexible and the carboxylate groups are oriented so that their bisectors are almost normal to the germanium surface. The electric potential applied between the germanium and platinum plates influences the adsorption phenomena. Effects of pH and temperature are also considered. A possible mechanism for the acid adsorption is proposed.

**Infrared Absorption Spectra of Alternating Copolymer of Butadiene with Acrylonitrile and Deuterated Analogues.** J. Furukawa, E. Kobayashi,

K. Uratani, Y. Iseda, J. Umemura, and T. Takenaka. *Polymer Journal*, **4**, 358 (1973).—Polarized IR spectra of alternating copolymers and random ones of butadiene with acrylonitrile have been investigated in the region from 4000 to 250  $\text{cm}^{-1}$ . The spectra of deuterated alternating copolymers have also been measured. It has been found that dichroism appears to a marked extent when films of the alternating copolymer are elongated, whereas it is hardly observable for the random one. The results were discussed from a viewpoint of orientation of polymer molecules and crystallites in the films of alternating copolymer. Tentative assignments of the absorption bands were made with reference to the results for *trans*-1,4-polybutadiene and those for polyacrylonitrile. The molecular structure of the alternating copolymer is discussed.

**Lattice Vibrations and Raman Band Splittings of Dipropionamide.**

K. Machida, Y. Kuroda, T. Uno, and S. Hayashi. *Spectrochim. Acta*, **30A**, 125 (1974).—The far-infrared and low-frequency Raman spectra of dipropionamide have been measured, and the lattice vibrational frequencies have been assigned on the basis of the infrared dichroism and the single crystal laser-Raman polarization measurement. The normal coordinate treatment has been made for optically active intra- and intermolecular vibrations of four molecules in the Bravais unit cell. The lattice vibrational frequencies are explained well by the force field including the hydrogen bond stretching force constant, which reflects the weakness of the bifurcated hydrogen bond, and non-bonded atom-atom repulsion constants. In order to reproduce the observed band splittings of intramolecular vibrations, it is necessary to introduce appropriate coupling constants between the equivalent internal symmetry coordinates of neighboring molecules. The origin of these coupling constants were discussed in relation to the dipole-dipole interaction.

**Analytical Electron Microscope.** E. Suito and H. Yotsumoto. *Ceramic Data Book* **57**, 77 (1974), in Japanese.—Review; various types of recent electron microscopes such as conventional and scanning electron microscope are reviewed. Principle and construction of analytical electron microscope was introduced.

**Elementary Layers in the Interstratified Clay Minerals as Revealed by Electron Microscopy.** T. Yoshida. *Clays and Clay Minerals*, **21**, 413 (1973).—Interstratified layer structures were studied by electron microscopy and electron diffraction. In order to distinguish between expansible and non-expansible layers, interstratified mica-smectite was treated with laurylamine hydrochloride solution. Electron micrographs of the layers at the curled edges of the crystals show expanded basal spacings of 24 Å and unexpanded spacings of 10 Å. It was observed that adjacent pairs of expanded and unexpanded layers in the micrographs form nonexpansible units. Arrangement of the expanded and unexpanded layers shows that the layers expanded by sorption of laurylammonium ions have expansible and non-expansible surface characteristics on opposite sides of the layer. The relationships between the ratio of component layers and basal spacings in two component systems are discussed.

**Effects of Spherical Aberration and Accelerating Voltage on Atomic Resolution in Molecular Images.** N. Uyeda and K. Ishizuka. *Journal of Electron Microscopy*, **23**, 79 (1974).—The anticipated molecular images of chlorinated-Cu-phthalocyanine were synthesized by computer simulation for four cases: 500 kV,  $C_s=1.0$  mm and 1.8 mm; and 100 kV,  $C_s=1.4$  mm and 0.35 mm; where  $C_s$  is the coefficient of spherical aberration for the objective lens. It was demonstrated that for 100 kV electrons even heavy atoms may not be recognizable unless  $C_s$  is less than 0.35 mm. Elevation of the accelerating voltage to 500 kV seems to be effective in obtaining atomic resolution, especially for the heavy atoms. Because through-focusing markedly changes the molecular images, there will be difficulty in the determination of molecular structures.

**Dynamic Properties of Powder and Particle Characteristics.** M. Arakawa. *Zairyo (Journal of the Society of Materials Science, Japan)*, **23**, 504 (1974), in Japanese.—Review; the dynamic properties of powder in a vibrating state has been discussed on the bases of particle characteristics.

**Correct Molecular Image Seeking in the Arbitrary Defocus Series.** N. Uyeda and K. Ishizuka. *8th International Congress on Electron Microscopy, Canberra*, **1**, 322 (1974).—The defocus of only a few tens angstroms greatly changes the molecular image giving rise to false results. For the real atomic resolution, a method to reconstruct the correct images has been devised. It involves two successive Fourier transforms, during which the data are processed with pupil-functions based on assumed defocus values  $\Delta f'$ . If the practical defocus value  $\Delta f$  coincides with  $\Delta f'$ , the reconstructed images involves no extraordinarily high peaks and negative regions. Thus, one can reconstruct the correct images even from a singular electron micrograph taken with any  $\Delta f$ .

**Micro-Structures of Interstratified Clay Minerals.** E. Suito, N. Uyeda, and T. Yoshida. *8th International Congress on Electron Microscopy, Canberra*, **1**, 496 (1974).—Weathering product of Ohya Stone was examined by high resolution electron microscopy and electron diffraction. Several Clay minerals were recognized including a mica clay which is very thin along the b-axis, an ordinary mica clay which is thin along the c-axis, montmorillonite and a small amount kaolinite. The fine structure in the stacking layers of mica clay and the regularity in the stacking of unite layers of montmorillonite were discussed on the basis of high resolution electron microscopoy.

**Twinning in Low Temperature Silver Selenide.** J. R. Günter, N. Uyeda, and E. Suito. *8th International Congress on Electron Microscopy, Canberra*, **1**, 526 (1974).—It is shown that the selenidation of thin silver films at elevated temperature is a topotactic reaction, caused by epitactic nucleation of high temperature silver selenide on the silver surface, followed by phase transformation to the low temperature phase. The occurrence of two or even three different orientations of the selenide, the preference of one of them in extended single crystalline areas, and the presence of prominent

planar defects in a specific orientation are qualitatively explained by geometrical arguments.

**Epitaxial Nucleation and Growth of Vacuum-Condensed Organic Semiconductor.** N. Uyeda, Y. Murata, and E. Suito. *8th. International Congress on Electron Microscopy, Canberra*, **1**, 692 (1974).—Thin films of bromanyl (Tetrabromopara-benzoquinone) are formed by vacuum condensation on KCl cleavage. These films assumes two different types of epitaxial relations to the substrate lattice, as found by the direct observation of lattice images of the crystallites. The mechanism of the epitaxial nucleation is discussed on the basis of the oriented adsorption of the individual molecules interacting with the surface lattice ions of the substrate.

**Can an Electron Microscope Reveal an Atom?** N. Uyeda. *Bussei*, **15**, 347 (1974), in Japanese.—The recent claim by several investigators that they succeeded in resolving atoms by a conventional electron microscope was criticised in view of the real meaning of resolution in atomic scale.

A straight forward principle to attain the resolution is explained on the basis of a series of computer simulation of molecular images which is associated with the newly constructed 500 kV electron microscope.

**Visualization of Molecular Structure.** N. Uyeda and K. Ishizuka. *Nihon-Denshikenbikyo-Gakkaishi-Kaiho*, **No. 12**, 10 (1974), in Japanese.—On the basis of computer simulation, it was demonstrated that the resolution of atomic scale cannot be attained for the electron microscopic images of organic molecules unless the spherical aberration coefficient of objective lens was reduced to about 0.35 mm for a conventional 100 kV electron microscope. It was also shown that the elevation of accelerating voltage up to 500 kV is useful for the atomic resolution even when the spherical aberration coefficient is improved to be about 1.8~1.0 mm. A new technique was proposed to seek an image which reflects the correct molecular structure even from a single image which was taken under an arbitrary defocussing of the objective lens.

**Powder Characteristics and Particle Size.** M. Arakawa. *Syokubai (Catalyst)*, **16**, 51 (1974), in Japanese.—Review; the effects of particle size on characteristics of powder were discussed and techniques of particle size measurement were reviewed.

## Inorganic Chemistry

**Separation of Heavy-Metal Ions from their Water Solutions by Xonotlite Crystal Compacts.** T. Maki and M. Ohkubo. *Bull. Inst. Chem. Res., Kyoto Univ.*, **51**, 278 (1973).—Compacts of Xonotlite crystal powders fired to temperatures ranging from 200° to 1000° C showed a great ability in separating heavy-metal ions from their water solutions and also fairly high compressive strengths even in the solutions. A mechanism of the separation of heavy-metal ions by the Xonotlite crystal compacts

was investigated, especially in copper sulphate solutions. When the Xonotlite crystal compacts is immersed in the copper sulphate solution,  $\text{Ca}^{2+}$  ions in the Xonotlite crystals dissolve into the solution. Increase in the pH of the solution causes the  $\text{Cu}^{2+}$  ions to precipitate as  $\text{Cu}_4(\text{SO}_4)(\text{OH})_6$  crystals on the surface of the fibrous crystals intercrossing each other in the compact.

#### **Identification of Crystals Protruding from Surface of $\text{Na}_2\text{O} \cdot 3\text{SiO}_2$ Glass.**

T. Yamamoto, K. Haraga, and M. Tashiro. *Bull. Inst. Chem. Res., Kyoto Univ.*, **51**, 305 (1973).—When a fresh fragment of  $\text{Na}_2\text{O} \cdot 3\text{SiO}_2$  glass was bombarded with intense electron beams, in an electron microscope, needle-shaped crystals, about 10 nm in diameter, grew out from the glass surface. When the fragment was allowed to stand in the air saturated with water for three weeks before subjected to the electron bombardment, a little curved rod-shaped crystal, about 200 nm in diameter, grew out from the glass surface. Electron diffraction analysis of the needle- and rod-shaped crystals indicated that the former crystals are  $\text{Na}_2\text{O}$ , the latter being  $\text{NaHCO}_3$ . These results were supported by in-situ observation of the crystals during heating up to  $800^\circ\text{C}$  under the electron microscope. Formation of these crystals was interpreted as one of the phenomena of percrystallization.

#### **Formation of Metastable Pyrochlore-Type Crystals in Glasses.**

T. Kokubo, S. Ito, and M. Tashiro. *Bull. Inst. Chem. Res., Kyoto Univ.*, **51**, 315 (1973).—Review; structures of metastable crystals in  $\text{K}_2\text{O}-\text{Ta}_2\text{O}_5-\text{Nb}_2\text{O}_5-\text{Al}_2\text{O}_3-\text{SiO}_2$  and  $\text{PbO}-\text{TiO}_2-\text{Al}_2\text{O}_3-\text{SiO}_2$  glasses as well as conditions of formation of the crystals were investigated to speculate the structures of the mother glasses.

#### **Recent Advances in Glass-Ceramics and their Application.**

M. Tashiro. *Ceramics*, **9**, 382 (1974), in Japanese—Review.

#### **Recent Development of Ferroelectric Glass-Ceramics.**

T. Kokubo. *Electronic Ceramics*, **6**, 9 (1974), in Japanese.—Review.

#### **Rate of Homogeneous Nucleation in Alkali Disilicate Glasses.**

K. Matsushita and M. Tashiro. *J. Non-Crystalline Solids*, **11**, 471 (1973).—Rates of crystal nucleation in alkali disilicate glasses were measured by counting the number of crystal under an optical microscope. The viscosities of these glasses were measured by the method of beam-bending and penetration. Using the data of rate of nucleation and viscosity obtained in the present study and the data of free energy measured by Takahashi and Yoshio, crystal-glass interfacial energies for alkali disilicate systems were estimated on the basis of homogeneous nucleation theory as follows:  $196 \text{ erg/cm}^2$  for  $\text{Li}_2\text{O} \cdot 2\text{SiO}_2$ ,  $126\text{--}144 \text{ erg/cm}^2$  for  $\text{Na}_2\text{O} \cdot 2\text{SiO}_2$  and  $88\text{--}104 \text{ erg/cm}^2$  for  $\text{K}_2\text{O} \cdot 2\text{SiO}_2$ . The effects of the viscosity of glass, the free energy difference between crystal and glass and crystal-glass interfacial energy on the rate of nucleation were discussed, and the remarkably higher rate of crystal nucleation in the  $\text{Li}_2\text{O} \cdot 2\text{SiO}_2$  glass was attributed to the larger free energy difference.

**Dielectric Properties of Fine-Grained  $\text{PbTiO}_3$  Crystals Precipitated in a Glass.** T. Kokubo and M. Tashiro. *J. Non-Crystalline Solids*, **13**, 328 (1973).—The spontaneous deformation of  $\text{PbTiO}_3$  crystals precipitated in a  $\text{PbO-TiO}_2\text{-Al}_2\text{O}_3\text{-SiO}_2$  glass was found to decrease with decreasing grain size. This trend remains even after the glass matrix surrounding  $\text{PbTiO}_3$  crystals is removed completely by  $\text{HNO}_3$  acid immersion. Consequently, a linear electro-optic effect cannot be expected from transparent glass-ceramics which necessarily comprise very-fine-grained crystals. The dielectric constant of  $\text{PbTiO}_3$  crystals surrounded by a glassy matrix shows two maxima at grain sizes  $0.15\text{ }\mu\text{m}$  and  $250\text{ }\text{\AA}$ , but is still fairly high even at a grain size as small as  $160\text{ }\text{\AA}$ . This suggests that a material with a large quadratic electro-optic effect may be produced from a transparent glass-ceramic. The maxima of the dielectric constant at grain sizes  $0.15\text{ }\mu\text{m}$  and  $250\text{ }\text{\AA}$  interpreted in terms of the internal stress and internal electric fields, respectively.

**Glass Formation in the Systems  $(\text{K or Cs})_2\text{O}-(\text{Nb or Ta})_2\text{O}_5\text{-Al}_2\text{O}_3$ .** T. Kokubo, M. Nishimura, and M. Tashiro. *J. Non-Crystalline Solids*, **15**, 329 (1974).—The glass-forming ability of melts in the systems  $\text{K}_2\text{O}-(\text{Nb and/or Ta})_2\text{O}_5\text{-Al}_2\text{O}_3$  as well as those in which  $\text{K}_2\text{O}$  was replaced with  $\text{Li}_2\text{O}$ ,  $\text{Na}_2\text{O}$ ,  $\text{Cs}_2\text{O}$ ,  $\text{BaO}$  or  $\text{PbO}$  was investigated. Some melts in the systems  $(\text{K or Cs})_2\text{O}-(\text{Nb and/or Ta})_2\text{O}_5\text{-Al}_2\text{O}_3$  could be made into glasses by cooling, yielding practically useful amounts. The structure of these glasses were discussed on the basis of their infrared spectroscopic and X-ray emission spectroscopic analyses.

**Effect of Added Oxides on the Crystallization of  $\text{Li}_2\text{O}\cdot 2\text{SiO}_2$  Glasses.** K. Matsushita and M. Tashiro. *Phys. Chem. Glasses*, **14**, 77 (1973).—Glasses of the compositions  $33.3\text{ Li}_2\text{O}\cdot 66.7\text{SiO}_2\cdot 3\text{RO}_n$  (mole ratio), where  $\text{RO}_n$  is an added oxide component, were heated from room temperature to various temperatures at a rate of  $5\text{ deg C/min}$ . The total number and the radius of crystal particles precipitated in each of the glasses were measured under an optical microscope and an electron microscope. The viscosities of the glasses were also measured. It was found that, except for the glasses containing  $\text{GeO}_2$ ,  $\text{P}_2\text{O}_5$ , and  $\text{V}_2\text{O}_5$ , the total number of crystal nuclei formed per unit volume of glass was inversely proportional to the viscosity at a temperature at which the rate of nucleation was nearly at its maximum; also the rate of crystal growth was found to be inversely proportional to the viscosity.

**Surface Structure of Glass-Ceramics.** T. Kokubo. *Hyomen*, **12**, 189 (1974), in Japanese—Review.

**Formation of a Metastable Pyrochlore-Type Crystal in  $\text{K}(\text{Ta, Nb})\text{O}_3$ -Containing Glasses and its Relation to Structure of the Glasses.** S. Ito, T. Kokubo, and M. Tashiro. *Yogyo-Kyokai-Shi* **81**, 327 (1973), in Japanese.—A metastable pyrochlore-type crystal with a composition presumably of  $\text{K}_{1.5}(\text{Ta}_{0.65}\text{Nb}_{0.35})\text{O}_{5.75}$  was found to precipitate in the  $\text{K}_2\text{O-Ta}_2\text{O}_5\text{-Nb}_2\text{O}_5$  glasses with addition of a small amounts of  $\text{Al}_2\text{O}_3$  and  $\text{SiO}_2$  on heating prior to precipitation of a stable



perovskite-type  $K(\text{Ta}, \text{Nb})\text{O}_3$  crystal. The pyrochlore-type crystal could be formed only by crystallization of the glasses, but not by ordinary solid state reaction of their raw materials. The X-ray diffraction pattern and infra-red spectrum of the mother glasses were both much alike to those of the pyrochlore-type crystal than those of the perovskite-type crystal. The structure of the glasses was considered to be composed of a random network of  $\text{TaO}_6$  and  $\text{NbO}_6$  octahedra and  $\text{K}^+$  ions being situated in some holes of the network.

**Rate of Crystal Growth in  $\text{Li}_2\text{O} \cdot 2\text{SiO}_2$  Glass.** K. Matusita and M. Tashiro. *Yogyo-Kyokai-Shi*, **81**, 500 (1973), in Japanese.—The rate of crystal growth in  $\text{Li}_2\text{O} \cdot 2\text{SiO}_2$  and  $33.3\text{Li}_2\text{O} \cdot 66.7\text{SiO}_2 \cdot 1.5\text{R}_2\text{O}$  ( $\text{R}$ ; Na, K, Cs) glasses were measured with a high temperature microscope set consisting of an ordinary polarizing microscope and a microfurnace having a very small heat capacity. It was deduced from the growth data that in  $\text{Li}_2\text{O} \cdot 2\text{SiO}_2$  glass lithium disilicate crystals grew with a screw dislocation mechanism and that the activation energy for diffusion across the crystal-liquid interface was equal to that for viscous flow of the melt. In  $33.3\text{Li}_2\text{O} \cdot 66.7\text{SiO}_2 \cdot \text{R}_2\text{O}$  glasses, lithium metasilicate as well as lithium disilicate crystals precipitated.

**Growth and Electrical Properties of  $\text{FeMe}_2\text{X}_4$  ( $\text{Me}=\text{Ti}, \text{V}$ ;  $\text{X}=\text{S}, \text{Se}$ ) Single Crystals.** S. Muranaka and T. Takada. *Bull. Inst. Chem. Res., Kyoto Univ.*, **51**, 287 (1973).—Single crystals of  $\text{FeMe}_2\text{X}_4$  ( $\text{Me}=\text{Ti}, \text{V}$ ;  $\text{X}=\text{S}, \text{Se}$ ) were grown by the isothermal vapor growth in the closed tube, using  $\text{Cl}_2$  or  $\text{TeCl}_4$  as a growth agency. The sizes of crystals produced were  $3 \times 2 \times 0.8$  mm— $10 \times 1 \times 0.8$  mm. The temperature dependence of electrical resistivity from 78 K to 350 K and the thermoelectric power at room temperature were measured on single crystals. These measurements showed that  $\text{FeMe}_2\text{X}_4$  exhibited metallic behaviors.

**Mössbauer Study of Some Barium Orthoferrates.** T. Ichida, Y. Bando, T. Shinjo, and T. Takada. *Bull. Inst. Chem. Res., Kyoto Univ.*, **51**, 295 (1973).—Mössbauer spectra were taken for the following barium orthoferrates,  $\text{BaFeO}_x$  ( $2.5 \leq x < 3.0$ ), at various temperatures between 4.2 K and 300 K: Triclinic-II, cubic-tetragonal and hexagonal phases were prepared by annealing or oxidizing the triclinic-I  $\text{BaFeO}_{2.5}$  at moderately low temperatures. Four kinds of  $\text{Fe}^{3+}$  internal field were observed in the spectra of the triclinic-I. Two kinds of  $\text{Fe}^{3+}$  and one kind of  $\text{Fe}^{4+}$  were detected in the triclinic-II. The spectrum for cubic-tetragonal had two 6-line splittings corresponding to  $\text{Fe}^{3+}$  and  $\text{Fe}^{4+}$  states respectively. The hexagonal sample also had two internal fields corresponding to  $\text{Fe}^{3+}$  and  $\text{Fe}^{4+}$  states and it was found that the transition from antiferromagnetic to paramagnetic gradually occurred between 125K and 171K.

**Role of Grain Boundary in Sintering and Electric Properties of Ceramics.** Y. Bando and T. Takada. *Electroceramics*, **11**, 24 (1973), in Japanese.—Review; the formation of grain boundary phase in sintering of some oxides was explained by liquid phase sintering mechanism and the effect of grain boundary phase on the electrical properties of ceramics were reviewed.

**Single Crystal Growth of CuO by Chemical Transport Method.** N. Yamamoto, Y. Bando, and T. Takada. *Japan. J. Appl. Phys.*, **12**, 1115 (1973).—CuO single crystal growth was performed using a chemical transport method. Obtained single crystals showed two kinds of crystal shapes depending on its preparation conditions.

**A Simple He<sup>3</sup>-Dilution Refrigerator.** K. Okada and T. Shinjo. *Japan. J. Appl. Phys.*, **12**, 1281 (1973).—A simple He<sup>3</sup>-dilution refrigerator for Mössbauer spectroscopy was manufactured by the present authors. Only 15 minutes were necessary for the cooling from 1.2K to 0.1K. Using a small heater, the sample could be kept at any temperature. The absolute temperature was estimated by the Co<sup>57</sup> Mössbauer thermometry.

**A New Preparation Method of Mn<sub>5</sub>O<sub>8</sub>.** N. Yamamoto, M. Kiyama, and T. Takada. *Japan. J. Appl. Phys.*, **12**, 1827 (1973).—Mn<sub>5</sub>O<sub>8</sub> was prepared using a new preparation method. Magnetic susceptibility was measured from liq. He to room temperature and this material was determined to be antiferromagnetic below 136 K.

**New Preparation Method and Metal Ion Distribution in CoMn<sub>2</sub>O<sub>4</sub>.** N. Yamamoto, S. Kawano, N. Achiwa, M. Kiyama, and T. Takada. *Japan. J. Appl. Phys.*, **12**, 1830 (1973).—CoMn<sub>2</sub>O<sub>4</sub> (tetragonal spinel) was prepared using a new preparation method. Metal distribution in this material was determined by neutron diffraction method. Results were as follows. Inversion parameter = 0.16 ± 0.01, Debye-Waller factor  $B = 1.0 \times 10^{-16} \text{ cm}^2$  and  $u = 0.230$  and  $v = 0.390$ .

**Single Crystal Growth of  $\alpha$ -MnO<sub>2</sub>.** N. Yamamoto, T. Endo, M. Shimada, and T. Takada. *Japan. J. Appl. Phys.*, **13**, 723 (1973).— $\alpha$ -MnO<sub>2</sub> single crystal was prepared using a high-pressure autoclave technique. Magnetic measurement was performed from liq. He to room temperature and this material was determined to be antiferromagnetic below 24.5K.

**Surface State of Ferromagnetic Cobalt Metal by Mössbauer Spectroscopy.** T. Shinjo, T. Matsuzawa, T. Takada, S. Nasu, and Y. Murakami. *J. Phys. Soc. Japan*, **35**, 1032 (1973).—Magnetic properties of ferromagnetic metal surface have been studied by Co<sup>57</sup> Mössbauer source measurements. On a surface of cobalt or copper, natural cobalt was electrolytically deposited and subsequently a microquantity of Co<sup>57</sup> was deposited under the same electrolytic condition. The Mössbauer spectrum at 4.2K showed that the hyperfine field of Fe<sup>57</sup> in the surface of cobalt has a distribution ranging from 260kOe to 350kOe. This result suggests that the magnetic moment in the surfaces does not differ greatly from the bulk value.

**The Magnetic Hyperfine Field at Co<sup>57</sup> in Antiferromagnetic CoO: A Mössbauer Study at Very Low Temperatures.** K. Okada and T. Shinjo. *J. Phys. Soc. Japan*, **36**, 1017 (1974).—The magnetic hyperfine field at Co<sup>57</sup> nucleus in

antiferromagnetic CoO was measured by Mössbauer experiments at very low temperatures. The sample was cooled down to 0.08K by a He<sup>3</sup>-dilution refrigerator. Then the nuclear polarization of the parent nucleus, Co<sup>57</sup>, occurred and the emission spectrum became to be asymmetric. From the intensity ratio of the outermost peaks it was derived that the sign of the hyperfine field was plus and the magnitude was  $590 \pm 40$  kOe. A considerable amount of Fe<sup>3+</sup> coexisted and the hyperfine field at Co<sup>57</sup> nucleus estimated from the Fe<sup>3+</sup> spectrum was  $603 \pm 80$  kOe.

**Mössbauer Study of the Thermal Decomposition Products of BaFeO<sub>4</sub>.**

T. Ichida. *J. Solid State Chem.*, **7**, 308 (1973).—A pure sample of a hexavalent iron compound, BaFeO<sub>4</sub>, was decomposed at temperatures below 1200°C at oxygen pressures from 0.2 to 1500 atm. In addition to the already known BaFeO<sub>x</sub> ( $2.5 \leq x < 3.0$ ) phases with hexagonal and triclinic symmetry, two new phases were obtained as decomposition products at low temperatures. One of the new phases, with composition BaFeO<sub>2.61-2.71</sub>, has tetragonal symmetry; lattice constants are  $a_0 = 8.54 \text{ \AA}$ ,  $c_0 = 7.29 \text{ \AA}$ . The phase is antiferromagnetic with Néel temperature estimated to be  $225 \pm 10$  K. Two internal fields observed on its Mössbauer spectra correspond to Fe<sup>3+</sup> and Fe<sup>4+</sup>. In the other new phase, with composition BaFeO<sub>2.5</sub>, all Fe<sup>3+</sup> ions had the same hyperfine field; it too is antiferromagnetic with a Néel temperature of  $893 \pm 10$  K. Mössbauer data on the hexagonal phase coincided with earlier results of Gallagher, MacChesney, and Buchanan [*J. Chem. Phys.*, **43**, 516 (1965)]. In the triclinic-I BaFeO<sub>2.50</sub> phases, internal magnetic fields were observed at room temperature, and it was supposed that there were four kinds of Fe<sup>3+</sup> sites. The phase diagram of BaFeO<sub>x</sub> system was determined as functions of temperature and oxygen pressure.

**Numerical Tables of Response Functions and their Integrals for Debye, Cole-Cole, and Davidson-Cole Types of Dielectric Relaxation.**

N. Koizumi and Y. Kita. *Bull. Inst. Chem. Res., Kyoto Univ.*, **50**, 499 (1972).—The theory of a transient current method for studying the dielectric properties in ultra-low frequency regions is discussed in connection with investigation of extremely slow relaxation processes. Numerical values of response functions and their integrals, which are needed for analysis of transient currents under application of step voltage and ramp voltage, are tabulated as a function of time for the Debye, Cole-Cole, and Davidson-Cole type of relaxations over wide ranges of time and of a distribution parameter of relaxation times.

**A Method for Estimating Residual Inductance in High Frequency A. C.**

**Measurements.** K. Asami, A. Irimajiri, T. Hanai, and N. Koizumi. *Bull. Inst. Chem. Res., Kyoto Univ.*, **51**, 231 (1973).—A new method was proposed to estimate residual inductance inherent in a specimen and its terminal leads in dielectric measurements. For a specimen specified by a capacitance and a resistance which are independent of measuring frequency, the product of capacitance and resistance as the readings of an a.c. bridge is to show a linear relation to the squared frequency. The

residual inductance can be calculated from the slope and the intercept of the linear relation. By the application of the method to parallel networks of a capacitor and a resistor with varied length of the terminal leads, reasonable results are obtained concerning the impedance per unit length of the leads. The method is also applied to a parallel plate cell system filled with salt solutions. The inductance evaluated for the cell system is seen to be varied with the conductance of the salt solution used. Comparison of the method is made with the Schwan method which was used to estimate the residual inductance.

**Dielectric Relaxation of Some Aliphatic Esters in Cyclohexane Solution.**

J. Crossley and N. Koizumi. *J. Chem. Phys.*, **60**, 4800 (1974).—The dielectric constant and loss data, measured at seven microwave frequencies, for seventeen aliphatic esters in cyclohexane solution at 25°C have been analyzed for mean relaxation times and Cole-Cole distribution parameters. The relaxation times for ethyl esters are slightly longer than those for corresponding methyl ester. In both cases, however, the relaxation time does not lengthen significantly as R in RCOOR' is increased from C<sub>5</sub> to C<sub>22</sub>. It would appear that the dielectric absorption of aliphatic esters is similar to that for aliphatic ketones and is dominated by an intramolecular relaxation process.

**Electrical Properties of Synaptosome Vesicles.**

A. Irimajiri, K. Kamino, N. Uyesaka, A. Inouye, and T. Hanai. *J. Physiol. Soc. Japan*, **35**, 381 (1973).—Measurements of dielectric constant and conductivity were made, between 0.5 and 250 MHz, on the suspension of synaptosomes isolated from rat brain cortex. The synaptosomal suspensions showed a typical dielectric dispersion which was critically dependent on the presence of a thin limiting membrane of extremely low conductivity. An analysis of the data based upon Pauly & Schwan's theory on a shell-sphere model revealed that electric conductivities for synaptosome interior changed with the external conductivities with a proportionality ratio of 0.37, that dielectric constants for the internal phase (27~35) were significantly lower than that for the external aqueous media (~75), but that synaptosomal membrane capacity remained constant ( $0.67 \pm 0.01 \mu\text{F} \cdot \text{cm}^{-2}$ ) irrespective of nature and concentration of the univalent salts examined (NaCl and KCl). The whole body of the results obtained was consistently interpreted by taking into consideration the presence of a substructure such as synaptic vesicles and small mitochondria inside the synaptosomal particles: under isotonic conditions about 50% of the internal volume might be occupied with a low conductivity substance like vesicles of lipidic nature provided that the intervesicular space was in equilibrium with the external salt media, a value of 50% being closely related to the osmotic dead volume for synaptosomes as reported previously.

**Physico-Chemical Properties of Thin Lipid Membranes.**

T. Hanai. *J. Japanese Chemistry (Kagaku no Ryooiki)*, Supplement, **103**, 25 (1973), in Japanese.—With respect to lipid black films formed in aqueous phases, the data reported in references are summarized on the physico-chemical properties such as the possibility of membrane formation, the electrical capacitance, the thickness the electrical resistance,

the permselectivity, the permeability of various kinds of materials, the change of permeation properties due to the addition of some antibiotics to the membranes.

**Permeation of Artificial Thin Films to Ions.** T. Hanai. *J. Japan Medical Association*, **70**, 1372 (1973), in Japanese.—Underwater bilayer lipid membranes have recently become a very significant model system for the study on reconstitution of functions of biological cell membranes. This article reviews the study of change of ion permeation corresponding to the different kinds of substances added to the membranes as a modifier of the membrane structure. The lipid membranes show relatively high electrical resistance and no permselectivity so far as the following substances are added: water soluble amino acids, lipophilic amino acids, globular proteins and lower-membered straight chain polypeptides. The addition of higher-membered straight chain polypeptides such as gramicidins, cyclic polypeptides such as valinomycin, nonactin, enniatins, and polyene antibiotics such as filipin and nistatin to the lipid membranes leads to the remarkable decrease in the electrical resistance and to the development of permselectivity.

**Bimolecular Lipid Membranes (Black Films).** T. Hanai. *J. Japan Oil Chemists' Soc.*, **21**, 289 (1972), in Japanese.—This treatise gives an outline of the study of bimolecular lipid membrane systems concerning the following items: historical survey, formation of the membranes, comparison of the membranes with biological cell membranes, permeation to ions and non-ionic substances, effect of amino acids, globular proteins and polypeptides on the permeation of the membranes and effect of enzyme-substrate reactions.

**Permeation of Reconstituted Membranes to Substances.** T. Hanai. *Clinic All-Round (Soogoo Rinsho)*, **21**, 96 (1972), in Japanese.—The treatise is an introductory review of the study of underwater lipid bilayer membranes, which are called reconstituted membranes because of some possibility of developing characteristics of biological cell membranes.

**The Comparison of Permeation Properties to Materials of Biological Cell Membranes and Artificial Films.** T. Hanai. *Kagaku Koogaku*, **38**, 413 (1974), in Japanese.—From the viewpoint of permeation to ions and molecules of biological relevance, a comparison is made between biological cell membranes and artificial membrane systems including lipid black films, millipore filters and synthetic high-polymer films as applied to artificial lung and kidney. In the field of chemical engineering, the permeation properties of synthetic polymer films to gases such as oxygen and carbon dioxide are successfully applied to the development of artificial lung. To a good extent, the permeation of synthetic polymer films to water, electrolytes, urea and some other materials can be controlled to be applicable to artificial kidney. The artificial control of the membrane transport of various kinds of biopolymer molecules is still left underdeveloped and is desired to be accomplished for the development of artificial organs.

**ESR Studies of Stable Free Radical Pairs in the Diamagnetic Matrix Crystal.** O. Takizawa, J. Yamauchi, H.O. Nishiguchi, and Y. Deguchi. *Bull. Chem. Soc. Japan*, **46**, 1991 (1973).—The radical pair system of a stable free radical, di-*p*-anisyl-nitric oxide (DANO), has been observed in the magnetically diluted crystal of 4,4-dimethoxy-benzophenone. The existence of the radical pair has been ascertained by the characteristic ESR absorptions, which give rise to the zero-field splitting and half-field resonance, of the powdered sample as well as by a comparison of the magnitude of the hyperfine coupling constants of the isolated radical with that of the pair system. The precise ESR measurements were performed using a single crystal containing 7.5% DANO radicals oriented well in the diamagnetic matrix. The fine structure parameters,  $|D|$  and  $|E|$ , have been determined to be 186 Gauss and 2 Gauss respectively, from which the distance between the two radical molecules in the pair system is estimated to be 5.4 Å. In order to deduce the structures of the radical pair, the *g*-value and hyperfine coupling constant of the isolated radical have been determined.

**The Magnetic Properties of Verdazyl Free Radicals. III. The Anomalous Magnetic Behavior of Symmetrical Triphenylverdazyl.** N. Azuma, J. Yamauchi, K. Mukai, H.O. Nishiguchi, and Y. Deguchi. *Bull. Chem. Soc. Japan*, **46**, 2728 (1973).—The static magnetic susceptibility and the ESR spectra from 1.6 to 300 K have been measured on a powder sample of the titled free radical. The broad maximum in the susceptibility which indicates an antiferromagnetic interaction has been observed at 6.9 K. The broadening of the ESR absorption line and the shift of the *g*-value have been found in the temperature region below  $T_{\max}$ , in which the susceptibility reached its round maximum. There appeared anomalies in the slope of the susceptibility, the linewidth, and the *g*-value *versus* temperature curves in the vicinity of 1.7 K. These anomalies may imply a magnetic-phase transition from the short-range ordered state to the long-range ordered state at about 1.7 K. The existence of a ferromagnetic interaction between the magnetic chains in the triphenylverdazyl radical solid is discussed on the basis of the susceptibility, the spin distribution, and the crystal structure. It is understood qualitatively that the radical with a negative spin density has a latent ferromagnetic interaction in or between the magnetic chains, and that the observation of this interaction greatly depends upon the molecular and crystal structure.

**Studies of the Equilibria between Tetraarylallyl-Type Radicals and their Dimers.** K. Watanabe, J. Yamauchi, H.O. Nishiguchi, and Y. Deguchi. *Bull. Chem. Soc. Japan*, **47**, 274 (1974).—Tetraarylallyl-type radicals are stable radicals. In these series, TPA (tetraphenyl allyl) is obtained as radical crystals. However, BDA, BDAA, and DDA radicals are obtained as diamagnetic dimerized substances. These are partially dissociated in solution. These can be detected in solution by ESR and optical spectra measurements of these radicals about the equilibrium between the radical monomer and its dimer. The equilibrium constants and the energy of the formation of the dimer are thus determined. The order of the magnitudes of the dimer's

formation energies can be explained in terms of the frontier electron densities of the bond-forming positions of radicals.

**Proton Magnetic Resonance in Organic Free Radicals, BDPA-Bz and *p*-Cl-BDPA.** K. Uchino, J. Yamauchi, H.O. Nishiguchi, and Y. Deguchi. *Bull. Chem. Soc. Japan*, **47**, 285 (1974).—The proton NMR absorption spectra from 1.3 to 77 K in two organic free radicals, BDPA-Bz and *p*-Cl-BDPA, have been measured on powder samples which undergo a magnetic phase transition from a paramagnetic to an antiferromagnetic state at the temperatures of 1.695 and 3.25 K respectively. The behavior of the NMR absorption spectra associated with the magnetic phase transition has been studied for the first time in the organic free radicals and interpreted in terms of the hyperfine interaction. These results are then compared with those of the TANOL radical, which is a linear antiferromagnet with no magnetic phase transition down to 1.3 K. It may be concluded that the intensity of the proton NMR absorption line decreases abruptly in the vicinity of the Néel temperature.

**Temperature Dependence ENDOR Spectra of  $\alpha,\alpha,\gamma,\gamma$ -Bisdiphenylene- $\beta$ -Phenyl Allyl Radical and its Derivatives.** K. Watanabe, J. Yamauchi, H.O. Nishiguchi, Y. Deguchi, and K. Ishizu. *Chem. Lett.*, 489 (1974).—ENDOR spectra of  $\alpha,\alpha,\gamma,\gamma$ -bisdiphenylene- $\beta$ -phenyl allyl radical (BDPA) and its derivatives have been observed and hyperfine splitting constants and spin density distribution have been determined. It was indicated that the unpaired electron spreads even to the aryl group attached to the  $\beta$ -position of the allyl skeleton of BDPA. The temperature dependence of the ENDOR spectra of these radicals was also studied. At low temperature below  $-85^\circ\text{C}$  the allyl skeleton twists unsymmetrically on either side and the wagging activation energy is estimated to be about 2.5 Kcal/mol.

**Magnetic Phase Transition of Organic Free Radical *p*-Cl-BDPA.** J. Yamauchi, K. Adachi, and Y. Deguchi. *J. Phys. Soc. Japan*, **35**, 443 (1973).—The heat capacity of polycrystalline organic free radical, *p*-Cl-BDPA, has been measured between 1.5 and 20 K. The broad maximum near 5 K in the magnetic heat capacity corresponds to the short range magnetic ordering of the unpaired electron. At 3.25 K a sharp peak was observed, which indicates paramagnetic-antiferromagnetic phase transition. The magnetic entropy of the transition yields 101.5% of the expected  $R\ln 2$ . A large fraction of the expected  $R\ln 2$  is consumed in the spin system above 3.25 K. This fact shows the low-dimensionality of the magnetic interaction in the organic free radical crystal, *p*-Cl-BDPA. Below  $T_N$  the magnetic heat capacity was in good agreement with the three-dimensional spin wave theory of antiferromagnet. The spontaneous sublattice magnetization as a function of temperature was evaluated as a following relation;  $M/M_0 = [1 - (T/T_N)^{3.9}]^{1/2}$ .

**Organic Free Radicals in Diamagnetic Matrices.** J. Yamauchi. *Kagaku no Ryoiki*, **27**, 1090 (1973), in Japanese.—This article described in Japanese contains in part a review concerning to the organic free radicals in diamagnetic matrices. The

anisotropy of  $g$ -values, hyperfine interaction and dipolar interaction parameters are precisely discussed in the organic stable free radicals. Discussion is divided into two problems, 1) isolated organic free radicals 2) inter-radical interactions in the diamagnetic matrices.

## Organic Chemistry

**The Reaction of Arylthallium (III) Compounds with Copper (II) and (I) Thiocyanates.** S. Uemura, S. Uchida, M. Okano, and K. Ichikawa. *Bull. Chem. Soc. Japan*, **46**, 3254 (1973).—Arylthallium (III) acetate perchlorates reacted with copper (II) thiocyanate to afford aryl thiocyanates in various solvents. The Cu (I) salt was found to be less effective for the thiocyanation. The choice of solvent and addition of potassium thiocyanate had a significant effect on the yield of aryl thiocyanates. The reaction with the mixture of copper (II) and potassium thiocyanates (1:1) in dioxane showed the best result. Electron-releasing groups in the aromatic ring accelerated hydrodethallation, yielding aromatic hydrocarbons with a depression of the thiocyanate formation.

**The Chlorobromination of Olefins with Antimony (III and V) Chlorides.** S. Uemura, A. Onoe, and M. Okano. *Bull. Chem. Soc. Japan*, **47**, 143 (1974).—By the reaction of olefins with equimolar mixtures of  $\text{SbCl}_5$  and  $\text{Br}_2$  or  $\text{LiBr}$ , and of  $\text{SbCl}_3$  and  $\text{Br}_2$ , in carbon tetrachloride, various bromochloroalkanes were obtained in good yields. The mixtures of certain metal chlorides of the Lewis acid type (e.g.,  $\text{FeCl}_3$ ,  $\text{SnCl}_4$ , and  $\text{TiCl}_4$ ) and  $\text{Br}_2$  could also be used as chlorobrominating agents, but these mixtures were found to be inferior to the  $\text{SbCl}_5$ - $\text{Br}_2$  mixture in product selectivities.

**Aromatic Bromination and Iodination with Mixtures of Antimony (V) Chloride and Halogens.** S. Uemura, A. Onoe, and M. Okano. *Bull. Chem. Soc. Japan*, **47**, 147 (1974).—Equimolar mixtures of  $\text{SbCl}_5$  and  $\text{Br}_2$  or  $\text{I}_2$  were found to be elegant reagents for the halogenation of certain aromatic substrates. In carbon tetrachloride, halogenobenzenes afforded the corresponding bromo- and iodo-derivatives with high *para*-selectivities (more than 95%) in good yields. The bromination of aromatic compounds with deactivating groups, such as ethyl benzoate and nitrobenzene, was simply achieved in 1,2-dichloroethane. Based on competitive halogenation data, the attack of  $\text{BrCl}$  or  $\text{ICl}$  (both formed *in situ*) on aromatics has been suggested.

**The Chlorination of Olefins with Antimony (V) Chloride.** S. Uemura, A. Onoe, and M. Okano. *Bull. Chem. Soc. Japan*, **47**, 692 (1974).—Antimony (V) chloride was revealed to be a good reagent for the *cis*-chlorination of simple olefins in chlorinated hydrocarbon solvents, such as 1,2-dichloroethane, dichloromethane, chloroform, and carbon tetrachloride. The higher the reaction temperature or the solvent polarity was, the higher the selectivity for *cis*-chlorination became. From



1,3-butadiene, *cis*-1,4-dichloro-2-butene was formed together with the *trans*-1,4- and 1,2-dichloro isomers. In the cases of cyclopentene and norbornene, the *trans*-1,2-dichloride and other various dichlorides were obtained without any formation of the *cis*-1,2-isomer. Probable mechanisms for this chlorination are briefly discussed.

**Synthesis of Alkoxythallium (III) Compounds of Olefins and their Reaction with Copper Halides and Pseudohalides.** S. Uemura, K. Zushi, A. Tabata, A. Toshimitsu, and M. Okano. *Bull. Chem. Soc. Japan*, **47**, 920 (1974).—Some new alkoxythallium (III) compounds of olefins,  $C_6H_5C(R^1)(OR^3)CH_2Tl(OCOR^2)_2$  [I], are prepared from styrene and  $\alpha$ -methylstyrene, with thallium (III) acetate and isobutyrate in various alcohols. I ( $R^1=H$ ) reacts with copper (I) iodide, bromide, chloride, cyanide and thiocyanate to afford the corresponding alkyl halides and pseudohalides,  $C_6H_5CH(OR^3)CH_2X$  (II), in various organic solvents, acetonitrile being the solvent of choice for the purpose of preparing II. The addition of potassium salt has a remarkable effect in improving the yield of II. The halo- and pseudohalo-dethallation occur at the position where thallium is attached previously to alkyl carbon. An ionic concerted intermolecular scheme is proposed as a reaction mechanism for the preparation of II. The data of NMR and IR spectra of I are briefly discussed.

**$\mu_3$ -Oxotrimetal Acetato-Complexes of Chromium, Manganese, Iron, Cobalt, Rhodium, and Iridium.** S. Uemura, A. Spencer, and G. Wilkinson. *J. Chem. Soc., Dalton Transactions*, 2565 (1973).—New pyridine- and  $\beta$ -picoline-containing oxo-centred complex ions  $[M_3^{III}O(CO_2Me)_6L_3]^+$ ,  $M=Cr, Mn, Fe, Co, Ph$ , and  $L=py$  and  $\beta$ -pic, were synthesized and their redox behavior studied electrochemically. There is evidence for reduced species in which the oxo-centred triangular structure is maintained in the case of the Mn, Fe, and Co complexes but these could not be isolated. For iridium, complexes  $[Ir_3^{III,III,IV}O(CO_2Me)_6L_3]^{2+}$  in which the metal atom is in the mean oxidation state  $3^{1/3}$  have also been characterised and shown to undergo reduction to the  $Ir^{III}$  species. Attempts to prepare oxo-centred complexes of Cu, Ag, Ni, Pd, Pt, and Mo were unsuccessful. The cobalt complex ion  $[Co_3O(CO_2Me)_6L_3]^+$  appears to be different from the other oxo-centred ions and a structure with both bridging and chelate acetato-groups is proposed.

**Terpenoids. XXVI. Structures of Lasiokaurinol and Lasiokaurinin, Two Novel Diterpenoids of *Isodon lasiocarpus* (Hayata) Kudo.** E. Fujita, M. Taoka, and T. Fujita. *Chem. Pharm. Bull. (Tokyo)*, **22**, 280 (1974).—On the basis of chemical and spectroscopic evidence, the structure and absolute configuration of lasiokaurinol isolated from *Isodon lasiocarpus* (Hayata) Kudo were established as *ent*-1 $\beta$ -acetoxy-7 $\beta$ , 20-epoxy-16-kaurene-6 $\alpha$ , 7 $\alpha$ , 14 $\alpha$ , 15 $\alpha$ -tetraol. The structure of another minor diterpenoid, lasiokaurinin, was proposed on the basis of spectroscopic evidence. Some chemical reactions confirmed its structure and relative stereochemistry.

**Biosynthesis of the Diterpenes Enmein and Oridonin from *ent*-16-Kaurene.** T. Fujita, S. Takao, and E. Fujita. *J. C. S. Chem. Comm.*, 434 (1973).—*ent*-

16-Kaurene was shown by tracer experiments to be incorporated into enmein and oridonin in *Isodon japonicus* Hara.

**Teucvin, a Novel Furanoid Norditerpene from *Teucrium viscidum* var. *Miquelianum*.** E. Fujita, I. Uchida, T. Fujita, N. Masaki, and K. Osaki. *J. C. S. Chem. Comm.*, 792 (1973).—The structure and absolute configuration of teucvin, a new norditerpene isolated from *Teucrium viscidum* var. *Miquelianum* were determined by an X-ray crystallographic analysis of the bromo-derivative and from some of its reactions. Thus teucvin was proved to have 19-norclerodane-type skeleton possessing a furan, a  $\gamma$ -lactone, and an  $\alpha\beta$ -unsaturated  $\gamma$ -lactone rings.

**Terpenoids. Part XXV. Structures and Absolute Configurations of Isodoacetal, Nodosinin, and Odonicin, Novel Diterpenoids of *Isodon japonicus*.** E. Fujita, M. Taoka, Y. Nagao, and T. Fujita. *J. C. S. Perkin I*, 1760 (1973).—On the basis of spectroscopic data and chemical evidence, the structure and absolute configuration of isodoacetal, nodosinin, and odonicin were established. The first two are B-secokaurene derivatives and the third is *ent*-6 $\alpha$ , 15 $\alpha$ -diacetoxy-7 $\beta$ , 20-epoxy-7 $\alpha$ -hydroxykaura-2,16-dien-1-one. Chemical interconversions between isodoacetal and nodosinin were accomplished.

**Terpenoids. Part XXVII. Structure and Stereochemistry of Ponicidin, a Diterpenoid of *Isodon japonicus*.** E. Fujita, M. Taoka, M. Shibuya, T. Fujita, and T. Shingu. *J. C. S. Perkin I*, 2277 (1973).—On the basis of chemical and spectroscopic (especially n.m.r.) evidence, ponicidin, a novel diterpene of *Isodon japonicus* Hara, was assigned the structure *ent*-7 $\beta$ , 20:14 $\beta$ , 20-diepoxy-1 $\beta$ , 6 $\alpha$ , 7 $\alpha$ -tri-hydroxykaur-16-en-15-one. The results of an o.r.d. determination established its absolute configuration.

**Terpenoids. Part XXVIII. Total Synthesis of Enmein.** E. Fujita, M. Shibuya, S. Nakamura, Y. Okada, and T. Fujita. *J. C. S. Perkin I*, 165 (1974).—Enmein is a major bitter principle of the leaves of *Isodon trichocarpus* Kubo and *I. japonicus* Hara, and its complicated B-secokaurene-type structure and absolute configuration were elucidated by cooperation of three Japanese research groups. The authors attempted its total synthesis and achieved their end. This paper reports the details of the procedure.

**Terpenoids. Part XXIX. Chemical Conversion of Enmein into an Important Relay Compound for its Total Synthesis.** M. Shibuya and E. Fujita. *J. C. S. Perkin I*, 178 (1974).—In this paper, the conversion of enmein into *ent*-3 $\beta$ , 20-epoxy-3-methoxy-17-norkaurane-6 $\alpha$ , 16 $\alpha$ -diol, an important relay compound in its total synthesis, is reported.

**Alkaloids of Lythraceae Plants.** E. Fujita. *Farumashia*, 9, 599 (1973), in Japanese.—This is a short review on our research works with the alkaloids of Lythraceous

plants.

**Addition Products Obtained from the Chlorination of 1, 2-Dichloronaphthalene.** H. Suzuki, M. Terakawa, and T. Sugiyama. *Bull. Inst. Chem. Res., Kyoto Univ.*, **51**, 373 (1973).—1,2-Dichloronaphthalene was chlorinated with molecular chlorine in chloroform. The products were composed of a mixture of polychloronaphthalenes, and 1,2,3,4-tetrachloro-1,2,3,4-tetrahydronaphthalenes. The stereochemistry of the addition products, two of the six possible tetrachlorides, was established by proton magnetic resonance spectroscopy. Main adduct melting at 73–74°C was found to have structure of either  $\epsilon$ - or still unknown  $\beta$ -configuration. Minor adduct melting at 103–104°C was found to have the structure of  $\alpha$ -configuration.

**A Convenient Laboratory Method for the Preparation of Thiophene-carbonitriles.** H. Suzuki, T. Iwao, and T. Sugiyama. *Bull. Inst. Chem. Res., Kyoto Univ.*, **52**, 561 (1974).—In hexamethylphosphoric triamide as a solvent, the reaction of iodothiophenes with CuCN under mild conditions (80–90°C, 2–3 hr, without catalyst) was found to substitute the iodine atom by a cyano group smoothly. This method is attractive for laboratory preparations of acid- and/or alkali-sensitive, or thermally unstable thiophenecarbonitriles. The procedure was applied to prepare thiophene-2-carbonitrile, 3-methylthiophene-2-carbonitrile, 5-chlorothiophene-2-carbonitrile, 5-bromothiophene-2-carbonitrile, thiophene-2,5-dicarbonitrile, and 3-methylthiophene-2,5-dicarbonitrile in 85, 84, 91, 32, 73, and 83% yields, respectively.

**Synthesis of Hydroxybenzyl Compounds.** H. Hayashi and S. Oka. *Bull. Inst. Chem. Res., Kyoto Univ.*, **52**, 514 (1974).—A one-step synthesis of 2-, and 4-hydroxybenzyl compounds from the corresponding acetoxybenzyl acetates is described. This convenient procedure gives hydroxybenzyl methyl ethers, N,N-diethylhydroxybenzyl amines, N-phenyl-hydroxybenzyl amines, hydroxybenzyl azides, hydroxybenzyl cyanides *etc.* in fair yields.

**Radical Addition Reactions to the Carbonyl Group. I. The Reaction of Aliphatic Aldehydes with Di-*t*-butyl Peroxide.** K. Maruyama, M. Taniuchi, and S. Oka., *Bull. Chem. Soc. Japan*, **47**, 712 (1974).—The thermal decomposition of di-*t*-butyl peroxide in aliphatic aldehydes has been carefully examined. *n*-Aldehydes and  $\beta$ -substituted aldehyde gave appreciable amounts of *sec*-alcohols in the reactions. *sec*-Alcohol arose from the addition of the alkyl radical to the carbonyl group of aldehyde.  $\alpha$ -Substituted aldehydes, however, did not give *sec*-alcohol, but instead gave considerable amounts of enol ether-aldehydes and dialdehydes. The addition of the alkyl radical to the carbonyl group and the decarbonylation of aldehydes were influenced remarkably by the structures of the aldehydes.

**Asymmetric Double Induction.** N. Baba, M. Muroi, J. Oda, and Y. Inouye. *Bull. Inst. Chem. Res., Kyoto Univ.*, **52**, 493 (1974).—Additivity of the free energy differences at transition states was tested in asymmetric double inductions involving the

systems of acrylate with carbalkoxydimethylsulfonium ylid, of acrylate with chloroacetate, of methacrylate with chloropropionate to give chiral cyclopropane products and of pyruvate with acetate to give citramalic acid, all with (—)-menthol used at chiral center. Experiments showed the hypothesis to be valid in systems which gave higher optical yields.

**Cyclopropanation via the Michael Addition.** K. Nishiyama, J. Oda, and Y. Inouye. *Bull. Inst. Chem. Res., Kyoto Univ.*, **52**, 499 (1974).—It was proved by means of product analysis and deuterium labelling that the base-catalyzed reaction of phosphoenolpyruvate with active methylene compounds proceeded *via* nucleophilic addition, 1,3-proton shift and intramolecular displacement in the intermediate Michael adduct carbanion, ultimately to give cyclopropane derivatives.

**Biostereochemistry of Histidine Metabolism. II. The Steric Course of Ammonia Elimination from L-histidine.** S. Sawada, A. Tanaka, Y. Inouye, T. Hirasawa, and K. Soda. *Biochim. Biophys. Acta*, **350**, 354 (1974).—[2-<sup>2</sup>H] Urocanic acid was obtained from the enzymatic reaction of racemic and stereoselectively labelled, DL-(+)-(3*S*): (3*R*)-[2,3-<sup>2</sup>H<sub>2</sub>] histidine with histase prepared from *Pseudomonas striata*. The stereochemistry of deamination was assigned to be a stereospecific *trans*-elimination including *pro-R* proton liberation from the C-3 position of L-histidine.

**Asymmetric Induction in the Allylic Rearrangement of Chiral Amine Oxide.** Y. Yamamoto, J. Oda, and Y. Inouye. *J. C. S., Chem. Comm.*, 848 (1974).—The [2,3]-sigmatropic rearrangement of (*R*)-*N,N*-dimethyl-3-(1-phenyl-*trans*-but-1-enyl) amine oxide to give (*S*)-*O-trans*-1-phenylbut-2-enyl-*N,N*-dimethylhydroxylamine was effected thermally with nearly complete transfer of chirality from tetrahedral carbon to trigonal carbon *via* a cyclic transition state conformation.

**Symmetry and Optical Activity of Organic Molecules.** J. Oda. *Kagaku (Chemistry)*, **29**, 15 (1974), in Japanese.—Review; numerical designations for stereoisomerism and chirality in organic molecules was discussed on the basis of group theory and topology.

**Introduction to Chemical Asymmetric Reactions.** Y. Inouye. *Kagaku Sosetsu*, **No. 4**, 33 (1974), in Japanese.—Review; a general survey and historical background of asymmetric reactions are given with special emphasis on the theory and factors affecting asymmetric reactions. The empirical rules, stereochemical models and mathematical treatments of asymmetric reactions are discussed.

**Diastereoface and Diastereotopos Differentiating Reactions.** Y. Inouye. *Kagaku Sosetsu*, **No. 4**, 51 (1974), in Japanese.—Review; discrimination between diastereotopic faces and sites in asymmetric syntheses are surveyed on the basis of the novel classification and the article covers the literatures from 1968 through 1973 June.

## Polymer Chemistry

**Stress Relaxation of Polymer Solutions under Large Strain: Elastic Recovery after Partial Stress Relaxation.** S. Ohta, Y. Einaga, K. Osaki, and M. Kurata. *Bull. Inst. Chem. Res., Kyoto Univ.*, **51**, 220 (1973).—Constrained elastic recovery of shear strain was measured after partial stress relaxation for a concentrated solution of polystyrene in chlorinated biphenyl. A constant torsional shear strain  $s$  was applied to the sample held in a cone-plate sample holder during the period of  $-t_1 < t < 0$ . Then the shear stress was removed by releasing the clamp tightening the cone so that the sample was allowed to undergo a torsional shear deformation by itself. The elastic recovery  $\tau_R(t, t_1, s)$  was evaluated from the rotation angle of the cone measured as a function of time  $t$ . It increased and approached the ultimate value  $\tau_R(\infty, t_1, s)$  more rapidly when the period of relaxation  $t_1$  was shorter. A large fraction of the original strain  $s$  was recovered only when the initial strain  $s$  as well as  $t_1$  was very small. The effects of varying  $t_1$  and  $s$  on  $\tau_R(\infty, t_1, s)/s$  were similar to those on the strain-dependent relaxation modulus  $G(t_1, s)$  (=stress at  $t=0$  divided by  $s$ ). When  $t_1$  was longer than a certain time  $\tau'_k$ , the ratio  $\tau_R = [\tau_R(\infty, t_1, s)/s]/\lim_{s \rightarrow 0} [\tau_R(\infty, t_1, s)/s]$  was independent of  $t_1$  and was approximately equal to the ratio  $G(t_1, s)/\lim_{s \rightarrow 0} G(t_1, s)$  for large  $t_1$ . It was concluded that the internal state of the sample after the application of large strain  $s$  may be reorganized in the period of  $\tau'_k$  independent of  $s$  and the shear stress as well as the elastic recovery for  $t_1 > \tau'_k$  may be described by linear viscoelasticity if an effective strain  $s_e = s\tau_R$  is employed in the place of the actual strain  $s$ .

**Excimer Formation in Solutions of Vinylaromatic Polymers.** H. Odani. *Bull. Inst. Chem. Res., Kyoto Univ.*, **51**, 351 (1973).—Excimer formation and fluorescence in solutions of vinylaromatic polymers have been reviewed. In fluorescence spectra of a number of polymer solutions lower energy band is assigned to fluorescence from an excimer state formed by the interaction of nearby chromophores on the same polymer chain. Mechanism of intramolecular excimer formation in polymer systems have been discussed in relation to local conformation and local motion of the polymer chain. Temperature dependence of fluorescence from fluid solutions of vinylaromatic polymers have also been discussed through kinetic considerations.

**Viscoelastic Properties of Dilute Polymer Solutions.** K. Osaki. *Advances in Polymer Science*, **12**, 1 (1974).—A review article on viscoelastic properties of dilute polymer solutions. The subjects covered are:

- 1) Statistical mechanical theories on viscoelasticity of dilute solutions of flexible polymers. Special care was taken to introduce various theories in the form appropriate for application.
- 2) Comparison of the theories with published experimental results. Applicability of the bead-spring model theories was assessed for various combinations of polymer-solvent and for solutions of branched polymers.

- 3) Experimental results on viscoelastic properties of dilute polymer solutions at very high frequencies. The shape of the relaxation spectrum was shown in detail and the values of intrinsic viscosity at the limit of very high frequency were listed for a few polymer-solvent combinations.

**Effect of Molecular Weight Distribution on Viscoelastic Properties of Polymers.** M. Kurata, K. Osaki, Y. Einaga, and T. Sugie. *J. Polym. Sci.: Polym. Phys. Ed.*, **12**, 849 (1974).—The effect of molecular weight distribution on mechanical properties of concentrated polymer solutions was studied by measuring creep compliance and complex modulus for solutions of binary blends of narrow distribution polystyrenes in chlorinated biphenyl. Two-step plateaus in the rubbery plateau region, as reported for undiluted polymer blends, were observed for concentrated solutions provided the molecular weights of component polymers differed greatly. The  $n$ th order blending law ( $n=1,2,3$ ) of Bogue *et al.* was simplified in form to compare with experimental results. As far as the present version of simplification was concerned, the cubic blending law was better than the quadratic one in describing viscoelastic properties of polymer blends. The cubic blending law reproduced closely the magnitudes of viscoelastic functions such as loss modulus and relaxation modulus but it was not able to predict the two-step plateaus, even when the ratio of molecular weights of components was as large as 10. It also provided a good approximation to reported results on the steady-state compliance  $J_{eb}^0$  for undiluted binary polymer blends and present results for solution blends. Since the cubic blending law in the simplified version was consistent with previous results on concentration dependence of the steady-state compliance for concentrated solutions of narrow distribution polymers, it gave a unified expression for the steady-state compliance of binary polymer blends and concentrated solutions of narrow distribution polymers.

**Creep Behavior of Polymer Solutions. IV. Polystyrene in Chlorinated Diphenyl below  $M_c$ .** Y. Einaga, K. Osaki, M. Kurata, T. Sugie, and M. Tamura. *Macromolecules*, **6**, 598 (1973).—The creep compliance was measured for concentrated solutions of polystyrenes of low molecular weights ( $M=1.98 \times 10^4$  and  $5.1 \times 10^4$ ) in chlorinated diphenyl. The ranges of concentration and temperature studied were  $0.5 < c < 0.7$  g/ml and  $0 < T < 70^\circ$ , respectively. The time-concentration reduction method was applied to the relaxation moduli which were calculated from the creep compliances at various concentrations. The reduction was applicable over the whole range of time scale except for the range of very long time for  $M=5.1 \times 10^4$ . The shift factor  $a_c$  at high concentrations depended on the molecular weight, reflecting the molecular weight dependence of the segmental friction coefficient  $\zeta$  in the polymer solutions. The free volume theory was applied to  $a_c$  to examine the properties of  $\zeta$ . It was revealed that the free volume theory may be applicable over a wide range of concentration for polystyrene in chlorinated diphenyl. The viscosity divided by  $\zeta$  was proportional to  $(cM)^{1.0}$  if the molecular weight dependence of  $\zeta$  was taken into account. The rubbery plateau region was absent in the relaxation moduli:

$M$  for calculation of theoretical values had to be about 60% higher than real  $M$ . The steady-shear compliance was approximately proportional to  $c^{-2}$  and was higher than the value predicted by the Rouse theory. These results were compared with dynamic properties of moderately concentrated solution of high molecular weight polystyrenes. The shape of the relaxation spectra kept on varying gradually down to low concentrations for the latter solutions and the rubbery plateau region was observed even at low concentrations.

**Light-Scattering Studies of a Polystyrene-Poly (Methyl Methacrylate) Two-Block Copolymer in Dilute Solutions.** H. Utiyama, K. Takenaka, M. Mizumori, and M. Fukuda. *Macromolecules*, **7**, 28 (1974).—Light-scattering measurements were made on a two-block copolymer of polystyrene and poly (methyl methacrylate) using benzene and toluene as the solvent that is isorefractive to poly (methyl methacrylate). The molecular weight of the sample was  $1.53 \times 10^6$  and its styrene content by weight was 0.38. Both the benzene and toluene solutions exhibited an anomalous angular dependence of the reciprocal scattering function at finite solute concentrations. A reasonable explanation to the anomaly is given in which a long-range spherically symmetric potential is used for interaction between polystyrene subchains. The mean-square distance between the centers of mass of two polystyrene subchains decreases with increase in polymer concentration, which causes the solutions to exhibit negative third virial coefficients. The mean-square radius in toluene of the polystyrene in the two-block copolymer was significantly larger than that of the homopolystyrene of equal molecular weight indicating the effect of the repulsive interaction between dissimilar segments.

**Infinite-Dilution Viscoelastic Properties of Randomly Branched Polystyrenes.** N. Nemoto, Y. Mitsuda, J. L. Schrag, and J. D. Ferry. *Macromolecules*, **7**, 253 (1974).—The storage and shear moduli of dilute solutions of randomly branched polystyrenes were measured by the Birnboim-Schrag multiple-lumped resonator at frequencies ranged from 100 to 6000 Hz. Arochor 1232 and o-xylene were used as solvents, and the range of concentration was 0.003 to 0.013 g per ml. Double logarithmic plots of intrinsic storage and loss shear moduli versus frequency were linear at low frequencies as expected from theory. By assuming a regular comb structure for the branched polymer, values of branch points per molecule  $f$  were calculated from the reduced intrinsic steady-state compliance which was evaluated from the plots. It was shown that the value of  $f$  thus calculated in compared well with that deduced from polymerization kinetics for polymers of low degrees of long-chain branching.

**Stress Relaxation of Polymer Solutions under Large Strain.** Y. Einaga, K. Osaki, M. Kurata, S. Kimura, N. Yamada, and M. Tamura. *Polymer Journal*, **5**, 91 (1973).—Shear relaxation moduli  $G(t,s)$  were measured for various strains  $s$  with a relaxometer of the cone-plate type for concentrated solutions of polystyrene in chlorinated biphenyl. The strain was varied from 0.34 to 25 shear units. The time-

temperature reduction method was applicable to the shear-dependent relaxation moduli over the temperature range studied (20–50°C) and the shift factor  $a_T$  was independent of  $s$ . When  $s$  was very large,  $\log G(t,s)$  decreased very rapidly with increasing time in two regions of  $t$  (two-step relaxation) while  $\log G(t,s)$  for small  $s$  dropped rapidly only at long times (one-step relaxation). The relative rate of decrease of  $G(t,s)$  with increasing  $s$  was independent of  $t$  when  $t$  was larger than a certain time,  $\tau_h$ . The maximum relaxation time  $\tau_m$  was independent of  $s$  while the corresponding strength of relaxation  $G_m$  was proportional to  $I_D^{-0.83}$  when  $s$  was large. Here  $I_D$  is the first invariant of strain.

**Stress Relaxation of Polymer Solutions under Large Strain: Application of Double-Step Strain.** K. Osaki, Y. Einaga, M. Kurata, N. Yamada, and M. Tamura. *Polymer Journal*, **5**, 283 (1973).—Stress relaxation was measured after application of a double-step shear strain on a concentrated solution of polystyrene in chlorinated biphenyl. The first shear strain  $s_1$  was applied to the sample in a cone-plate sample holder of a relaxometer at time  $-t_1$ , the second strain  $s_2$  was added at  $t=0$ , and then the stress was measured as a function of time  $t$ . Ranges of  $s_1$  and  $t_1$  were 1.71–20.5 shear units and 10–5000 sec, respectively, while  $s_2$  was kept constant at 1.88 s.u. These results, together with published results for strain-dependent relaxation moduli, were employed to assess a group of constitutive equations which use single integrals with respect to the time  $t'$  to describe the strain history. It was shown that such constitutive equation could not in general describe the observed results, when invariants at  $t'$  of the strain rate of the strain were employed in the response functions to represent the nonlinear behavior. However, in the special cases of relatively small  $s_1$  or large  $t_1$ , constitutive equations of the single integral type described quantitatively the observed nonlinear behavior, when invariants of strain were employed in the response functions.

**Flow Properties of Polymer Solutions. I. Temperature Dependence of Stresses Following Sudden Start and Cessation of Steady Shear Flow.**

K. Osaki, Y. Einaga, N. Yamada, and M. Kurata. *Polymer Journal*, **6**, 72 (1974).—Following sudden start and cessation, respectively, of steady shear flow, stresses,  $\kappa\bar{\eta}(t, \kappa)$  and  $\kappa\tilde{\eta}(t, \kappa)$  were measured for a 20% solution of polystyrene in chlorinated biphenyl. Here  $\kappa$  is the rate of shear and  $t$  is the time after sudden change of rate of shear. Measurements were performed at every 5°C starting from 30°C up to 50°C with a rheometer of the cone-and-plate type in the range of rate of shear  $1 \times 10^{-4} \sim 5 \times 10^{-2} \text{ sec}^{-1}$ . Measured results included behaviors characteristic of high rates of shear such as stress overshoot as well as those characteristic of low rates of shear. The accuracy of data as examined with linear viscoelasticity relations at low rates of shear was satisfactory. A method of reduced variables with respect to temperature  $T$ , time  $t$ , and rate of shear  $\kappa$  was revealed to apply to stress development function  $\bar{\eta}(t, \kappa)$  and stress decay function  $\tilde{\eta}(t, \kappa)$ :  $\bar{\eta}(t, \kappa)/\eta^0$  and  $\tilde{\eta}(t, \kappa)/\eta^0$  obtained at various temperatures were unique functions of two variables  $t/a_T$  and  $\kappa a_T$ , where  $\eta^0$  is the zero-shear viscosity and  $a_T$  is the shift factor usually employed in the time-temperature reduction



for functions in linear viscoelasticity.

**Flow Properties of Polymer Solutions. II. Phenomenological Relation for the Stress Following Sudden Starts of Steady Shear Flow.** K. Osaki, Y. Einaga, N. Yamada, S. Ohta, and M. Kurata. *Polymer Journal*, **6**, 165 (1974).—The stress development at the start of steady shear flow was calculated from experimental data for the strain-dependent relaxation modulus of a concentrated polymer solution with the use of a constitutive equation based on the strain-dependent relaxation spectrum. Calculated results were in close agreement with those observed in the range of relatively low rate of shear, where no stress overshoot at the start of steady shear flow was observed. When stress overshoot was present, the calculated result was in close agreement with the observed up to the time at which the stress reached its maximum value. This time corresponded to a certain value  $s_B$  of the shear strain, irrespective of the rate of shear, and was accurately predicted from the relaxation modulus using the strain-dependent constitutive model. At longer times the calculated result for the rate of decrease of the stress overshoot was too small, compared with the observed, so that the predicted peak of the stress overshoot was too broad. It was concluded that the strain-dependent constitutive model may be applied to polymer solutions when the shear strain is smaller than  $s_B$  or when the rate of shear is smaller than  $s_B/\tau_m$ , where  $\tau_m$  is the maximum relaxation time of the polymer solution.

**Flow Properties of Polymer Solutions. III. Non-Newtonian Viscosity and Relaxation Mechanisms with Long Relaxation Times.** K. Osaki, Y. Einaga, N. Yamada, and M. Kurata. *Polymer Journal*, **6**, 179 (1974).—Contributions of relaxation mechanisms with long relaxation times were examined for the shear stress  $\kappa\tilde{\eta}(t, \kappa)$  after a sudden stop of steady shear flow of a 20% polystyrene solution in chlorinated biphenyl, where  $\kappa$  is the rate of shear and  $t$  is the time of stress decay. The longest relaxation time  $\tau_m(\kappa)$  and the corresponding strength  $\eta_m(\kappa)$  were evaluated from the slope and the intercept at  $t=0$ , respectively, of the asymptotic straight line at large  $t$  in the plot of  $\log \tilde{\eta}(t, \kappa)$  vs.  $t$ . Those for the second longest relaxation time,  $\tau_{m-1}(\kappa)$  and  $\eta_{m-1}(\kappa)$ , were obtained in a similar manner from the plot of  $\log [\tilde{\eta}(t, \kappa) - \eta_m e^{-t/\tau_m}]$  vs.  $t$ . The relaxation times  $\tau_m(\kappa)$  and  $\tau_{m-1}(\kappa)$  were found to be independent of  $\kappa$  and the ratio  $\tau_m(\kappa)/\tau_{m-1}(\kappa)$  was about 3. At the limit of zero rate of shear,  $\eta_m(\kappa)$  and  $\tau_{m-1}(\kappa)$  were approximately 30 and 45%, respectively, of the zero shear viscosity  $\eta^0$ . As  $\kappa$  increased,  $\tau_m(\kappa)$  and  $\eta_{m-1}(\kappa)$  decreased more rapidly than the steady shear viscosity  $\eta(\kappa)$  did; the difference  $\eta(\kappa) - \eta_m(\kappa) - \eta_{m-1}(\kappa)$  was almost independent of  $\kappa$ . It was concluded that the nonlinear behavior, such as the shear-dependent viscosity of the polymer solution, is mainly due to the nonlinear behavior of the few relaxation mechanisms with long relaxation times.

**Compositional Heterogeneity and Molecular Weight Distribution of Copolymer Systems. I. Simple Statistical Analysis of the Heterogeneities of Block and Graft Copolymers.** T. Kotaka, N. Donkai, and T. I. Min. *Bull. Inst. Chem. Res., Kyoto Univ.*, **52**, 332 (1974).—Expressions of various average molecular

weights including light-scattering apparent values, compositional heterogeneity and molecular weight distribution have been derived for block and graft copolymers by applying, respectively, the random-coupling, and the random-grafting statistics. The average molecular weights may be correlated with certain easily accessible experimental data. The relations provide important criteria for checking the heterogeneity of the material under investigation.

In particular it was shown that the complete description of compositional heterogeneity and molecular weight distribution may be obtained from the following experimental data:

- i) The overall chemical composition.
- ii) Molecular weight distributions of constituent homopolymers, *i.e.*, for a block copolymer those of the two precursor homopolymers, and for a graft copolymer those of the backbone prepolymer and of the graft-side-chains which may or may not be identical to that of the ungrafted side-chain homopolymer separable from the reaction mixture.
- iii) For a graft copolymer the true graft ratio or the grafting efficiency.
- iv) And for a mixed block copolymer the type and the relative amount of each species involved, which may be deduced from the reaction mechanism and kinetics.

**Some Fundamental Properties of Developer Solvents in Thin Layer Chromatography Applied to Polymer Separations.** F. Kamiyama and H. Inagaki. *Bull. Inst. Chem. Res., Kyoto Univ.*, **52**, 393 (1974).—To establish widely applicable rules to choose a developer appropriate for adsorption thin layer chromatography (TLC) of any given polymer sample, a variety of vinyl polymers have been chromatographed with different single and binary solvent on silica gel thin layers. Rules thus deduced are; (i) a chosen developer should be a solvent of sample polymer; (ii) a general theory proposed by Snyder for adsorption chromatography serves as a great help for the purpose. In addition, the development characteristics of binaries, which appears in adsorption TLC of polymers, is investigated experimentally in respect to the molecular weight dependence of  $R_f$  (rate of flow).

**The Separation and Characterization of Side Chain Polymers in Cellulose-Styrene Graft Copolymers.** T. Taga and H. Inagaki. *Angew. Makromol. Chem.*, **33**, 129 (1973).—Three cellulose-styrene graft copolymers were prepared by heterogeneous mutual polymerization technique, initiated by gamma-rays at a constant dose rate for different time intervals. The cellulose grafts were subjected to extraction with boiling benzene to remove the attendant homopolystyrene (PS), and then the cellulose backbones were degraded by acid hydrolysis. Each PS residue after hydrolysis has been separated with a thin layer chromatography (TLC) into two components: one involves some sugar residues due to hydrolysis at one of the chain ends, whereas the other does not. The former and latter components separated from a PS residue (PS-II) were denoted as PS-II (l) and PS-II (u), respectively. By making further use of TLC, the weight fraction of these components for each graft product has

been determined, which allowed assessment of the per cent grafting due to true grafting. It is pointed out how difficult is the extraction of homopolymer from graft product.

Number and weight average molecular weight,  $M_n$  and  $M_w$ , of PS-II, PS-II(1) and PS-II(u) have been determined by gel permeation chromatography, and others. The results indicated that  $M_w$  found for PS-II was much higher than that for PS produced in solution. Another finding was that  $M_w$  for PS-II (1), *i.e.*, truly grafted PS, was unexpectedly larger than that for PS-II(u), despite these polymers were formed both simultaneously inside the substrate. Further it was found that the molecular weight distribution of PS-II was appreciably broad, but this did result from a superposition of two fairly narrow distributions for PS-II (1) and PS-II (u). The grafting frequency for a cellulose graft prepared at a total dose of 2 Mrads was assessed to be 0.03 by using necessary data obtained so far.

**Ultracentrifuge Study of Critically Branched Polycondensates. II. Molecular Weight Measurements by the Archibald Method.** H. Suzuki and C. G. Leonis. *Br. Polym. J.*, **5**, 485 (1973).—Archibald molecular weight determinations were carried out on model polycondensate obtained near the gel point of decamethylene glycol and benzene 1,3,5-triacetic acid after stabilization of the carboxyls with diphenyl diazomethane and hydroxyls with ketene. The apparent molecular weights  $M_{app}(t)$ , estimated at the meniscus, decreased rapidly with time. This is in accord with a theoretical prediction. In the low concentration range examined, use of the Rayleigh interference fringes alone enabled us to evaluate the apparent molecular weights at early run times with fair reliability. Using semi-logarithmic plots of  $M_{app}(t)$  *vs.* the effective run time  $t$ , difficulty in extrapolation to  $t=0$  was not serious. The results were compared with those of earlier work on this model polycondensate system.

**Thin-Layer Chromatographic Separations of Butadiene-Styrene Copolymers on the Basis of Composition and Molecular Weight.** T. Kotaka and J. L. White. *Macromolecules*, **7**, 106 (1974).—Experimental methods have been developed for thin-layer chromatographic (tlc) separation of butadiene-styrene copolymers according to (i) composition and (ii) molecular weight. The technique of separation according to composition is based upon exploiting the adsorption of polymers from their solutions with less polar solvents through the greater adsorptivity of the relatively polar styrene units. The specific method involved is an elution gradient procedure based upon addition of a good relatively polar solvent for both polymers ( $\text{CHCl}_3$ ) to the nonpolar solvent  $\text{CCl}_4$ . Adsorption onto silica gel during the development increases with styrene content so that high  $R_f$  values are associated with low styrene contents. The separation method for determining molecular weight distributions is based upon using solvents of marginal solubility and involves adding a highly polar nonsolvent to an initial polar solvent which precipitates the polymer during the development. Specifically  $\text{CH}_3\text{OH}$  is used as the nonsolvent and a  $\text{CH}_3\text{OH}$ -tetrahydrofuran mixture is the initial solvent. Methods of quantitatively interpreting the TLC smears to obtain compositional heterogeneity and molecular weight distribution are described. De-

tailed calculations for several copolymers are included.

**Intermolecular Correlation in Light-Scattering from Dilute Solutions of Block Copolymers.** T. Tanaka, T. Kotaka, and H. Inagaki. *Macromolecules*, **7**, 311 (1974).—The effects of intermolecular correlation on scattered light intensities from block copolymer solutions were examined from the point of view of the distribution function theory developed by Zimm, Albrecht, and Flory and Bueche for homopolymer solutions. The theory predicts distorted Zimm plots for block copolymer solutions with solvents having nearly zero refractive index increment for one of the parent homopolymers. A larger distortion is expected, if the unmasked portion is much smaller relative to the overall dimension of a whole molecule, and if the deviation of the center of mass of the unmasked portion from the molecular center of mass is larger. Thus an AB-diblock copolymer would give a larger distortion, while a BAB-triblock copolymer a smaller distortion, if compared under the same conditions. On the basis of the theory a method was proposed for analyzing radii of gyration of block copolymer molecules by using the Guinier type plots. Series of block copolymers of polystyrene and poly(methyl methacrylate) were prepared anionically. Light-scattering measurements were made on these samples. The results were found to be in agreement with the predictions of the theory. An anomalous concentration dependence of scattered light intensities found in this study is also reported.

**Ultracentrifuge Study of a Critically Branched Polycondensate.** H. Suzuki, C. G. Leonis, and M. Gordon. *Makromol. Chem.*, **172**, 227 (1973).—Gelation may be brought about reversibly in weakly bonded polyfunctional systems, or irreversibly in strongly bonded ones. In either case, gelation is a critical phenomenon of striking sharpness. The critically branched state near to, and on either side of, the gel point gives rise of remarkable physical properties. For instance, this is the state of matter, in which life processes are generally observed.

Irreversible bonding processes have been studied in a model polyester of benzene 1,3,5-triacetic acid (BTA) and decamethylene glycol (DMG) by chemical kinetics and rheological measurements. Stabilization of the products, obtained by stopping the bonding process just before gelation, was achieved by converting the remaining carboxyls to benzhydryl ester with diphenyl diazomethane (DDM) and the free hydroxyls to acetyl ester by means of ketene.

Ultracentrifuge experiments were carried out on this critically branched and stabilized polycondensate of BTA/DMG/DDM/K in 2-butanone: it was found that the sedimentation constant  $S_0$  was 76 Svedberg and the weight-average diffusion constant  $D_{w,0}$  was  $3.5 \times 10^{-6}$  cm<sup>2</sup>/sec. The combination of large  $S_0$  and larger  $D_{w,0}$  is unfamiliar but easily explicable. Moreover the combination of large size and high mobility is reminiscent of a prerequisite for a medium in which life processes are to occur.

**Separation of *trans*-1,4 *cis*-1,4 and 1,2-Vinyl Polybutadienes by Thin Layer Chromatography.** N. Donkai, N. Murayama, T. Miyamoto, and H. Inagaki. *Makromol. Chem.*, **175**, 187 (1974).—A study on thin layer chromatographic (TLC)

separation of polybutadienes with three different microstructures, namely, *trans*-1,4, *cis*-1,4, and 1,2-vinyl, was carried out. An experimental procedure to separate three possible binary mixtures of these polymers into each component species is established in an alternate use of carbon tetrachloride and amyl chloride as developer. Further it is shown that this procedure combined with a two-dimensional TLC development technique allows to separate the ternary polymer mixture into components. In addition, the chromatographic behavior of so-called "equibinary" polybutadienes has been investigated using the technique established so far.

**Rheological Properties of Solutions of Butadiene-Styrene Copolymers of Varying Microstructure.** T. Kotaka and J. L. White. *Trans. Soc. Rheology*, **17**, 587 (1973).—An experimental study of the non-Newtonian viscosity  $\mu$  and principal normal stress difference  $N_1$  of solutions of polybutadiene, polystyrene, and their copolymers of varying microstructure has been carried out in decalin, decane and their mixtures. Decane is a non-solvent for polystyrene and a poorer solvent for polybutadiene than decalin. For the homopolymers and random copolymers, the viscosity and Weissenberg number ( $N_1/\sigma_{12}$ ) at constant shear rate decrease as non-solvent is added. For block copolymers, the opposite is observed. This is due to the polystyrene segments precipitating out in poor solvents and forming intermolecular aggregates. The SBS block copolymers tend to form viscoelastic gels because a three-dimensional network with polystyrene crosslinks is formed. The simple SB block copolymers show thixotropic behavior with yield stress. This may be explained by the two phase structure being in the form of micelles in which the polystyrene aggregates are solubilized by the polybutadiene segments.

**Polyelectrolyte Complexes I. Ionic Bonding between Sulfated and Aminoacetalized Derivatives of Polyvinyl Alcohol.** M. Hosono, O. Kusudo, S. Sugii, and W. Tsuji. *Bull. Inst. Chem. Res., Kyoto Univ.*, **52**, 442 (1974).—Interaction between a pair of poly-ion-compounds, sulfated and aminoacetalized derivatives of polyvinyl alcohol was studied by nephelometry under various conditions. In the turbidity curve of the mixing solution of the poly-ion-compounds, a maximum or minimum was observed at a position nearly equal to the stoichiometric equivalent. It is found that when the mixing proportion differs from the equivalent, the composition of the ion-complex produced somewhat varies according to the rate of stirring. A mechanism of the complex formation under the stirring is proposed.

**The Preparation of a New Type of Synthetic Fiber from Linear Polyethylene by Irradiation Cross-Linking.** R. Kitamaru, C. Tsuchiya, and S.-H. Hyon. *Bull. Inst. Chem. Res., Kyoto Univ.*, **52**, 436 (1974).—A lightly cross-linked polyethylene filament was obtained by a conventional melt-spinning and an irradiation with an electron beam from Van de Graaff. This cross-linked filament was stretched to a high extent in the perfectly molten state at high temperatures above its melting temperature and quenched. Through these procedures a new type of synthetic fiber having high melting temperatures as well as excellent mechanical and fiber

properties was prepared. The fiber obtained did not shrink appreciably if boiled in water for more than two hours and holded its fiber properties.

**Size and Orientation of Crystallites in Lightly Cross-Linked Polyethylene, Crystallized from the Melt under Uniaxial Compression.** R. Kitamaru and S.-H. Hyon. *Makromol. Chem.*, **175/1**, 255 (1974).—If lightly cross-linked polyethylene films are crystallized from the melt under uniaxial compression, a very unique alignment of the molecular chains in the crystalline phase of the samples appears. The orientation of crystallites in which the (200) crystal plane is located parallel to the film surface first appears at a relatively low degree of compression, and subsequently the orientation in which the (110) crystal plane is located parallel to the film surface follows at higher degrees of compression.

Despite the fact that the samples were crystallized from the melt rather rapidly, the unitcell density of the crystalline phase was very close to unity and the size of crystallites was very large. The dimensions of crystallites in the direction perpendicular to the film surface were in a range of 170–350 Å but they were as large as more than 1500 Å in the direction parallel to the film surface. Thus it is confirmed in addition by electron microscopic observation that these samples have a new type of lamellar structure in which molecular alignments are quite different from those for the so-called lamellar structure for polyethylene crystallized under isotropic conditions.

**Thermal Analysis of Acrylic Acid-Grafted Polypropylene Fabrics**  
(II) **Thermogravimetry.** T. Ikeda, W. Tsuji, and Y. Ikeda. *Sen-i Gakkaishi*, **29**, T-267 (1973), in Japanese.—Thermogravimetry of polypropylene ( $\leq 500^\circ\text{C}$ , heating rate  $10^\circ\text{C}/\text{min.}$ ) showed that weight loss of the polypropylene fabrics started at  $\sim 350^\circ\text{C}$  and  $220^\circ\text{C}$  in nitrogen and air, respectively. Thermogravimetric curves of acrylic acid-polypropylene graft copolymer fabrics showed that the initial degradation temperature (IDT) was lowered and degradation of the acrylic acid-polypropylene graft copolymer fabrics increased with increasing acid graft percentage on the polypropylene fabrics. Plotting IDT values of the polypropylene fabrics against the corresponding graft percentage gave a straight line.

**Dynamic Properties of Acrylic Acid-Grafted Polypropylene.** T. Ikeda, M. Hamanaka, Y. Ikeda, and W. Tsuji. *Sen-i Gakkaishi*, **29**, T-330 (1973), in Japanese.—The primary peak of the dynamic loss modulus of polypropylene monofilaments grafted with acrylic acid and treated with metal salts or tris (1-aziridinyl)-phosphine oxide (APO) measured at  $-20$  to  $+200^\circ\text{C}$ , shifted towards higher temperature and decreased in intensity with increasing acid grafting. The crystalline absorption of the polypropylene at  $110^\circ\text{C}$  was broadened by decreasing acid grafting, but well defined absorption peak appeared at  $140^\circ\text{C}$  with increasing grafting. The crystalline absorption of the grafted polypropylene shifted to high temperature and decreased in intensity with treatment with metal salt. Dynamic modulus ( $E'$ ) of the acid-grafted polypropylene treated with metal salt or APO decreased in the vicinity of melt-dispersion of polypropylene, though somewhat increased by the grafting and treatment with metal

salts or APO below this temperature. The APO-treated polypropylene had higher  $E'$  than untreated polypropylene or metal salt-treated polypropylene at 36.9% acid grafting.

**Chemical Modification of Synthetic Fiber by the Graft Copolymerization of Vinyl Monomer Having Functional Group-----Acrylic Acid-Grafted Polypropylene Fiber.** T. Ikeda. *Sen-i Gakkaishi*, **29**, T-395 (1973), in Japanese.—Review.

**Carboxymethylation of Cotton Fabrics by One Step Method.** R. Fujimoto N. Wakasaki, M. Hosono, and W. Tsuji. *Sen-i Gakkaish*, **30**, T-273 (1974), in Japanese.—A new processing for the carboxymethylation of cotton fabrics was studied. In order to prevent the byreaction of chloroacetic acid to glycolic acid, the cotton fabrics were first immersed in a mixed aqueous solution of sodium chloroacetate and sodium hydroxide at low temperatures and then carboxymethylated by heating. Some properties of the fabrics carboxymethylated by this procedure under different conditions were examined. It was found by these examinations that the cotton fabrics were carboxymethylated more uniformly than by conventional methods.

This new method is considered to be useful for the continuous carboxymethylation of cotton fabrics.

**Carboxymethylation of Cotton Fabrics by Glycolic Acid.** R. Fujimoto and W. Tsuji. *Sen-i Gakkaishi*, **30**, T-280 (1974), in Japanese.—Partial carboxymethylation of cotton fabrics was examined using glycolic acids and sulfuric acid, phosphoric acid, or acetic acid as acidic catalyzers. It was found that the reaction of this procedure gave a partially carboxymethylated cellulose having the crystalline lattice of cellulose I, whereas the usual method used to date where the reaction was achieved in the chloroacetic acid-sodium hydroxide system gave crystalline lattice of cellulose II.

**Improvement of Crease Resistance of Cotton Fabric by the Grafting with Acrylic Acid and Aftertreatment with Tris (1-aziridinyl) Phosphine Oxide.** T. Ikeda, Y. Ikeda, S. Ito, and W. Tsuji. *Sen-i Gakkaishi*, **30**, T-292 (1974), in Japanese.—Crease recovery of cotton fabric grafted with acrylic acid and further treated with tris (1-aziridinyl) phosphine oxide (APO) was studied with a view of preventing the decrease of tensile strength accompanied with crosslinking. Although the chemical structure of reaction products of APO with acrylic acid-grafted cotton is more complicated owing to the presence of the carboxyl groups in the grafted polyacrylic acid than that of the reaction products of APO with ungrafted cotton, APO seems to react not only with hydroxyl groups in the cotton cellulose, as observed for the ungrafted cotton, but also with carboxyl groups in the grafted cotton fabric. Crease recoveries of ungrafted and grafted cotton fabrics in both conditioned and wet states are much improved by treating with APO solution containing 2.5% zinc fluoroborate catalyst. Considerable crease-proofing effect is also observed when the grafted cotton fabrics

are treated with APO solution without zinc fluoroborate catalyst, and the decrease in the warp tensile strength is prevented by this treatment. This method is particularly favorable to obtain a good crease recovery-strength relationship.

**Some Problems in Structural Formation during Melt Spinning.** K. Katayama, T. Amano, and K. Nakamura. *Appl. Polymer Symp.*, **20**, 237 (1973).—The general feature of structural formation during melt spinning is discussed on the basis of experimental results. The process of crystallization during melt spinning is considered to be a nonisothermal crystallization under constant tension. Molecular orientation just before the onset of crystallization determines the microstructure of spun fibers. For a thorough prediction of the process of melt spinning, an analysis of melt flow is required from both the rheological and structural aspects. Isothermal melt spinning experiments were carried out and the birefringence and flow properties were analyzed by using a Jeffreys model. The stress-optical coefficient was estimated at  $1.5 \times 10^{-10}$  cm<sup>2</sup>/dyne for low density polyethylene from the experimental data. Problems to be solved in the strain-induced crystallization are discussed briefly.

**Some Aspects of Nonisothermal Crystallization of Polymers. III. Crystallization during Melt Spinning.** K. Nakamura, T. Watanabe, T. Amano, and K. Katayama. *J. Appl. Polym. Sci.*, **18**, 615 (1974).—Crystallization during melt spinning is studied as an example of the nonisothermal crystallization of polymers. The following equation is derived, taking the temperature distribution within a filament into consideration:

$$\kappa \nabla^2 T = V \cdot \text{grad } T - \frac{\Delta H}{C_p} V \cdot \text{grad } X$$

where  $T$ =temperature,  $X$ =crystallinity,  $\kappa$ =thermal diffusivity,  $V$ =velocity,  $\Delta H$ =heat of crystallization, and  $C_p$ =specific heat at constant pressure. The assumptions and the procedure for a numerical calculation of crystallinity and temperature within a running filament are described, and some results of calculation are illustrated. The results are compared with those obtained by a simpler calculation in which the radial temperature distribution is neglected. The simpler method proved useful in connection with X-ray measurements.

## Biochemistry

**Studies on L-Lysine Decarboxylase from *Bacterium Cadaveris*.** M. Moriguchi, T. Yamamoto, and K. Soda. *Bull. Inst. Chem. Res., Kyoto Univ.*, **51**, 333 (1973).—Crystalline L-lysine decarboxylase was obtained from the cell-free extract of *Bacterium cadaveris* grown in the medium containing L-lysine as an inducer. The purification was carried out by the several steps including heat treatment, ammonium sulfate fractionation, the first DEAE-Sephadex chromatography, Sepharose 4B gel filtration, and the second DEAE-Sephadex chromatography. The purified enzyme

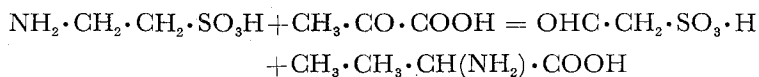


was crystallized by addition of ammonium sulfate. The crystals took the form of small rod. The crystalline enzyme is homogeneous by the criteria of ultracentrifugation ( $S_{20,w}^0=21.1$  S). The molecular weight is about 1,000,000, assuming a partial specific volume of 0.74. The spectrum of the enzyme exhibits two absorption maxima at 280 m $\mu$  and 425 m $\mu$ ; these give an absorbance ratio of 12:1. No appreciable spectral shifts occurred when pH (5.8–9.0) was varied.  $\delta$ -Hydroxylysine (DL and DL-allo) and *S*-( $\beta$ -aminoethyl)-L-cysteine are decarboxylated by the enzyme at a rate of 35 and 49% that for L-lysine, respectively. The enzyme, when examined in the presence of acetate and phthalate buffers, has an optimum reactivity at pH 5.8. The  $K_m$  are  $3.7 \times 10^{-4}$  M for L-lysine and  $4.5 \times 10^{-3}$  M for *S*-( $\beta$ -aminoethyl)-L-cysteine. The enzyme was found to contain 10 moles of pyridoxal 5'-phosphate per mole. The activity of enzyme was not influenced by the addition of  $\alpha$ -keto acid.

#### Occurrence of Taurine-Pyruvate Aminotransferase in Bacterial Extract.

S. Toyama, K. Miyasato, M. Yasuda, and K. Soda. *Agr. Biol. Chem.*, **37**, 2939 (1973).—The enzymatic transamination between taurine and pyruvate was demonstrated in the cell-free extract of *Pseudomonas* sp. (F-126) grown in the medium containing  $\beta$ -alanine (0.3–1.0%) and peptone (0.2%). Cells grown in the medium without  $\beta$ -alanine produced almost no detectable enzyme activity. The addition of pyridoxal 5'-phosphate to the reaction system caused little increase in the activity.

The transamination reaction was shown to proceed stoichiometrically. The reverse reaction was also observed when sulfoacet-aldehyde and L-alanine were used as the substrates. Thus, the good evidence was obtained for the occurrence of the new  $\omega$ -aminotransferase catalyzing transamination between taurine and pyruvate in the cell-free extract of *Pseudomonas* sp. (F-126) as follows.



#### Properties of Crystalline Kynureninase from *Pseudomonas marginalis*.

M. Moriguchi, T. Yamamoto, and K. Soda. *Biochemistry*, **12**, 2969 (1973).—The distribution of microbial kynureninase (L-kynurenine hydrolase, EC 3.7.1.3) among various strains was investigated and *Pseudomonas marginalis* was found to have the highest activity of enzyme, which was induced by the addition of L-tryptophan to the medium. The kynureninase was purified and crystallized from *Ps. marginalis*. The purified enzyme is homogeneous by the criteria of ultracentrifugation ( $S_{20,w}^0=5.87$  S) and disc gel electrophoresis. The mol. wt. is 100,000; assuming a partial specific volume of 0.74. The enzyme exhibits absorption maxima at 280, 337, and 430 m $\mu$ . No appreciable spectral change was observed on varying the pH between 5.4 and 9.0. The holoenzyme can be resolved to the apoenzyme by incubation with hydroxylamine, L-alanine, and L-ornithine, and reconstituted by the addition of pyridoxal 5'-phosphate. One mole of pyridoxal 5'-phosphate is bound per mole of enzyme. The formyl group of pyridoxal 5'-phosphate is bound in an aldimine link to the  $\epsilon$ -amino group of a lysine residue of the protein. The enzyme exhibits maximum reactivity

at about pH 8.0; it is stable over the pH range 5.8–8.0. Neither D-kynurenine nor N-formyl-L-kynurenine is hydrolyzed by the enzyme. The Michaelis constants were determined as follows: L-kynurenine,  $3.5 \times 10^{-5}$  M, and pyridoxal 5'-phosphate,  $2.3 \times 10^{-7}$  M (0.065 M Tris-HCl buffer, pH 8.0). The enzyme activity was inhibited by carbonyl reagents and thiol reagents.

**Transamination Reaction Catalyzed by Kynureninase and Control of the Enzyme Activity.** M. Moriguchi and K. Soda. *Biochemistry*, **12**, 2974 (1973).

—The inactivation of kynureninase occurred when the reaction was carried out in the absence of added pyridoxal 5'-phosphate. The degree of inactivation increased with the reaction time. The addition of either pyridoxal 5'-phosphate or pyruvate protected the enzyme from inactivation. Kynureninase was also inactivated by L-alanine, a reaction product, or by L-ornithine. The activity is restored by the addition of pyridoxal 5'-phosphate. Spectrophotometric studies on the inactivation indicate that the addition of L-alanine or L-ornithine to the holoenzyme leads to loss in the peaks at 337 and 430 m $\mu$ , and appearance of a new peak at 325 m $\mu$ . Apoenzyme was obtained by dialysis of L-ornithine-(or-L-alanine)-treated enzyme. The apoenzyme is reactivated by pyridoxamine 5'-phosphate plus pyruvate, or by pyridoxal 5'-phosphate. Thus, the inactivation is due to formation of the bound pyridoxamine 5'-phosphate from the bound pyridoxal 5'-phosphate by transamination with L-alanine or L-ornithine. The product from L-ornithine was identified as  $\Delta^1$ -pyrroline-2-carboxylic acid, the intramolecularly dehydrated form of  $\alpha$ -keto- $\delta$ -aminovaleric acid. Kynureninase catalyzes an overall transamination between L-ornithine and pyruvate. There is close correlation between the amino acids that cause inactivation and those that transaminate, and between the  $\alpha$ -keto acids that reactivate the inactivated enzyme and those that transaminate. The enzyme can act as an  $\alpha$ -aminotransferase of high substrate specificity to regulate the enzyme activity by interconversion of the coenzyme moiety.

**Biostereochemistry of Histidine Metabolism. II. The Steric Course of Ammonia Elimination from L-Histidine.** S. Sawada, A. Tanaka, Y. Inouye,

T. Hirasawa, and K. Soda. *Biochim. Biophys. Acta*, **350**, 354 (1974).—[2- $^2$ H] Urocanic acid was obtained from the enzymatic reaction of racemic and stereoselectively labeled, DL-( $\pm$ )-(3S): (3R)—[2,3- $^2$ H $_2$ ] histidine with histidase prepared from *Pseudomonas striata*. The stereochemistry of deamination was assigned to be a stereospecific trans-elimination including *pro*-R proton liberation from the C-3 position of L-histidine.

**Studies on Utilization of Fermentation and Respiration Energy to Biosynthetic Processes. I. Fermentative Production of Phosphoric Acid Anhydrides and Phosphate Esters.** T. Tochikura, Y. Kariya, T. Yano, and T.

Tachiki. *Amino Acid Nucleic Acid*, **29**, 59 (1974), in Japanese.—A fermentation process by use of a coupling by energy transfer was designed. The first step was the accumulation of FDP during fermentation of glucose by yeasts under high  $P_i$  concentrations and the second step was accomplished by coupling the fermentation of FDP with an ender-

gonic reaction through an ADP-ATP system.

Phosphorylations of several organic compounds were investigated with fermentation of FDP by yeasts. When dried baker's yeast of 50 mg/ml was incubated for several hours with media containing (per ml) FDP 40–80  $\mu$ mol,  $\text{MgSO}_4$  30  $\mu$ mol, adenosine, AMP, GMP, UMP or CMP 50  $\mu$ mol, at high potassium phosphate (pH 7.0) concentration of  $8 \times 10^{-1}$  M, the corresponding nucleoside polyphosphates (ATP, GTP, UTP or CTP) were produced in good yields of higher than 80 %. The production of GTP, UTP and CTP at higher  $\text{P}_i$  concentrations were strikingly accelerated by the addition of catalytic amounts of adenosine, AMP or ATP. Glucosamine 6-phosphate was found to be produced in good yields by coupling the phosphorylation of glucosamine with the yeast fermentation of FDP.

Phosphorylation of higher concentrations of nucleoside monophosphates were investigated with fermentation of glucose by baker's yeast. A maximum yield of UTP was found to be about 90  $\mu$ mol/ml/8hr with a medium containing (per ml)  $\text{P}_i$  800  $\mu$ mol, glucose 600  $\mu$ mol,  $\text{MgSO}_4$  30  $\mu$ mol, UMP 100  $\mu$ mol, AMP or ATP 5  $\mu$ mol and dried yeast 100 mg. At higher  $\text{P}_i$  concentration ( $8 \times 10^{-1}$  M), a maximum rate for the accumulation of UTP was about 30  $\mu$ mol/100 mg dried yeast/ml/2hr. The relationship between the phosphorylation of nucleoside monophosphate and the metabolism of FDP in the yeast was discussed.

The production of 6-phosphogluconate (6-PG) by use of a coupling by microbial energy transfer was investigated. The reaction consisted of two coupled reactions, the phosphorylation of ADP to form ATP by way of yeast fermentation of sugars and the phosphorylation of gluconate by gluconokinase of *coli-aerogenes*.

At first, 6-PG was found to be produced by the combination of cell-free extracts of baker's yeast as an ATP-generating source and ammonium sulfate ( $\text{AmSO}_4$ ) saturation 45–75 % fractions of *A. aerogenes* as a gluconate-phosphorylating source. The energy for coupling was supplied by the yeast fermentation of FDP at lower concentration of  $\text{P}_i$  ( $1 \times 10^{-1}$  M) and by the fermentation of glucose at higher concentration of  $\text{P}_i$  ( $3 \times 10^{-1}$  M). Additions of larger amounts of the cell-free extract of yeast to the  $\text{AmSO}_4$  fraction of *A. aerogenes* decreased the yields of 6-PG.

It was indicated that the ratio of sugar-fermenting activities of the yeast against gluconokinase activities of *A. aerogenes* was a very important factor for 6-PG production. Furthermore, the production of 6-PG various combinations of cell preparations of the yeast and *A. aerogenes* was investigated and its good yield were obtained under the following conditions: in the presence (per ml) of  $\text{P}_i$  800  $\mu$ mol, adenosine 5  $\mu$ mol, glucose 800  $\mu$ mol, gluconate 300  $\mu$ mol, the gluconokinase preparation 9.6 mg protein and the dried yeast 100 mg, 6-PG yield was about 240  $\mu$ mol (66 mg as free acid)/ml/11hr; in  $\text{P}_i$  600  $\mu$ mol, ATP 5  $\mu$ mol, glucose 600  $\mu$ mol, gluconate 200  $\mu$ mol, *A. aerogenes* 20–40 mg cells and the yeast 50–100 mg cells, 6-PG yields were 100–160  $\mu$ mol/3–5 hr.

#### **Fermentative Production of CDP-Choline-Related Compounds (Part**

1). Y. Kariya, K. Aisaka, A. Kimura, and T. Tochikura. *Amino Acid and Nucleic Acid*, 29, 75 (1974), in Japanese.—Fermentative production of CDP-choline and CDP-

choline-related compounds by yeasts was investigated. CDP-choline was produced in good yields from CMP and choline at high levels of inorganic phosphate under the condition of glucose catabolism by dried cell preparations of *Hansenula jadinii* IFO 0987.

CDP-choline production falls markedly by use of the older cells grown for long periods, because of inactivation of choline kinase and CDP-choline pyrophosphorylase. On the other hand, the high activity of CMP phosphorylation was observed with the old cells. At the condition of high concentration of CMP, the phosphorylation of CMP to CTP took place rapidly but the production of CDP-choline was not accelerated.

Presence of high concentration of CTP in the reaction mixture caused the inhibition of choline phosphorylation and this inhibitory effect was demonstrated by using the partially purified choline kinase from *H. jadinii*.

Feeding of small amounts of CMP and glucose to the reaction system, which started in low levels of CMP, accelerated CDP-choline production, and the final yield reached to the level of fermentation which P-choline.

Using the N-methyl or N-ethyl analogues of choline, production of corresponding CDP-esters was attempted. Remarkable amounts of CDP-esters except CDP-ethanolamine was produced. CDP-dimethylethanolamine was separated and isolated from the reaction mixture by ion exchange column chromatography and then crystallized as its sodium salt from alcoholic solution.

**Enzymatic Properties of Bacterial Crystalline Kynureninase.** M. Moriguchi, T. Yamamoto, and K. Soda. *Amino Acid and Nucleic Acid*, **29**, 143 (1974), in Japanese.—The distribution of microbial kynureninase (L-kynurenine hydrolase EC 3.7.1.3) among various strains was investigated and *Pseudomonas marginalis* was found to have the highest activity of enzyme, which was induced by the addition of L-tryptophan to the medium. The kynureninase was purified and crystallized from *Ps. marginalis*. The purified enzyme is homogeneous by the criteria of ultracentrifugation and disc gel electrophoresis. The molecular weight is 100,000 assuming a partial specific volume of 0.74. The enzyme exhibits absorption maximum at 280, 337, and 430 nm. No appreciable spectral change was observed on varying the pH between 5.4 and 9.0. The holoenzyme can be resolved to the apoenzyme by incubation with hydroxylamine, L-alanine, and L-ornithine, and reconstituted by the addition of pyridoxal 5'-phosphate. The formyl group of pyridoxal 5'-phosphate is bound in an aldimine link to the  $\epsilon$ -amino group of a lysine residue of the protein. The enzyme exhibits maximum reactivity at about pH 8.0; it is stable over the pH range 5.8~8.0. The Michaelis constants were determined as follows; L-kynurenine,  $3.5 \times 10^{-5}$  M, and pyridoxal 5'-phosphate,  $2.3 \times 10^{-7}$  M (0.065 M Tris-HCl buffer, pH 8.0). The enzyme activity was inhibited by carbonyl reagents and thiol reagents.

**Regulatory Mechanism of Kynureninase Activity by the Transamination Reaction of the Bound-Coenzyme.** M. Moriguchi and K. Soda. *Amino Acid and*

*Nucleic Acid*, **29**, 150 (1974), in Japanese.—The inactivation of kynureninase occurred when the reaction was carried out in the absence of added pyridoxal 5'-phosphate. The degree of inactivation increased with the reaction time. The addition of pyridoxal 5'-phosphate or pyruvate protected the enzyme from inactivation. Kynureninase was also inactivated by L-alanine, a reaction product, or by L-ornithine. The activity is restored by the addition of pyridoxal 5'-phosphate. Spectrophotometric studies on the inactivation indicate that the addition of L-alanine or L-ornithine to the holoenzyme leads to loss in the peaks at 337 and 430 nm, and appearance of a new peak at 325 nm. Apoenzyme was obtained by dialysis of L-ornithine-(or L-alanine)-treated enzyme. The apoenzyme is reactivated by pyridoxamine 5'-phosphate plus pyruvate, or by pyridoxal 5'-phosphate. Thus, the inactivation is due to formation of the bound pyridoxamine 5'-phosphate from the bound pyridoxal 5'-phosphate by transamination with L-alanine or L-ornithine. The product from L-ornithine was identified as  $\Delta^1$ -pyrroline-2-carboxylic acid, the intramolecularly dehydrated form of  $\alpha$ -keto- $\delta$ -aminovaleric acid. Kynureninase catalyzes an overall transamination between L-ornithine and pyruvate. There is close correlation between the amino acids that caused inactivation and those that transaminate, and between the  $\alpha$ -keto acids that reactivate the inactivated enzyme and those that transaminate. The enzyme can act as an  $\alpha$ -aminotransferase of high substrate specificity to regulate the enzyme activity by interconversion of the coenzyme moiety.

**On the Transamination Reaction of Taurine with Pyruvate in the Cell Suspension of a Soil Bacterium.** S. Toyama, K. Miyasato, T. Toma, and K. Soda. *The Science Bulletin of the College of Agriculture, The University of Ryukyus*, **20**, 105 (1973), in Japanese.—This paper presents the enzyme catalyzing the transamination of taurine with pyruvate in the bacterial cell suspension of W-64 strain, which utilizes taurine as a sole carbon and nitrogen source.

1. The transaminase activity of the cells was enhanced greatly by addition of  $\beta$ -alanine to the growth medium.
2. In the enzyme reaction, both taurine and pyruvate as a substrate were required to produce  $\alpha$ -alanine. The formation of  $\alpha$ -alanine proceeded linearly as a function of incubation time and cell concentration. Pyruvate was one of the best amino acceptors. The pH optimum of the reaction was around 8.0.
3.  $\beta$ -Alanine-grown cells also catalyzed the transamination reaction of  $\gamma$ -aminobutyrate,  $\beta$ -alanine,  $\epsilon$ -aminocaproate, and taurine in this order with pyruvate.

**Amino Acid Racemases.** K. Soda. *Seikagaku*, **46**, 203 (1974), in Japanese.—The history, distribution, assay methods, cofactor requirement, and the enzymological and physicochemical properties of amino acid racemases were reviewed.

In particular the reaction mechanism and the regulatory mechanism of enzyme activity were discussed from the viewpoint of chemistry of pyridoxal phosphate enzymes. Some comments on the metabolic function of the enzymes were also given here.

**Restriction Endonucleases AP, GA, and H-I from Three *Haemophilus* Strains.** M. Takanami. *Methods in Molecular Biology*, (ed. R.B. Wickner), Marcel Dekker Inc., New York, **Chap. 5**, 113 (1974).—Restriction endonucleases which cleave double-stranded DNA at different sequences have been isolated from three *Haemophilus* strains. This article deals with the procedures for purification and the cleavage site specificities of these enzymes.

**DNA Sequence Restricted by Restriction Endonuclease AP from *Haemophilus Aphiophilus*.** H. Sugisaki and M. Takanami. *Nature New Biology*, **246**, 138 (1973).—The cleavage site specificity of a restriction endonuclease from *Haemophilus aphiophilus* has been determined. This enzyme introduces duplex cleavages on double-stranded DNA at the following sequence: — — — C/C G G — — —  
— — — G G C/C — — —.

**Flexibility of Tertiary Structures of Proteins: Lysozyme and Myoglobin.** M. Oobatake and T. Ooi. *Bull. Inst. Chem. Res., Kyoto Univ.*, **52**, 456 (1974).—Flexibility in Lysozyme and Myoglobin was examined by simple methods, one calculating displacements of  $C^\alpha$  atoms due to small variation of dihedral angle  $\varphi$  (N- $C^\alpha$  bond) and  $\psi$  ( $C^\alpha$ -C' bond), and the other, first derivatives of total energy by using a tentative repulsive potential between two residues. Since a large displacement of a distance in the negative direction (negative maximum displacement) for an interacting pair, or a large value of first derivative represents occurrence of atomic collision, we can infer the flexibility of each residue. The results show that the flexibility for  $\varphi_k$  is almost identical as for  $\psi_{k-1}$  in the opposite direction and terminal regions are more flexible than the rest in the molecule, the range being wider in C-terminal than in N-terminal for both proteins.

**Comparison of Homologous Tertiary Structures of Proteins.** K. Nishikawa and T. Ooi. *J. Theor. Biol.*, **43**, 351 (1974).—Homology in sequences of proteins which have the same or similar function has been studied as a problem of comparative biochemistry and molecular evolution. It is therefore of interest to examine homology in three-dimensional structures, e.g. whether folding of polypeptides having common residues gives rise to the same tertiary structure or not. Two methods, a difference map and a superposition technique, were used to evaluate the similarity in tertiary structures of proteins; hemoglobin  $\alpha$ -chain,  $\beta$ -chain, and myoglobin;  $\alpha$ -chymotrypsin and elastase. The results show that homologous folding of homologous chains is found for sequences of internal residues, while discrepancies occur mostly at surface regions, and some portions having common residues do not have the same structure. Another spatial homology was found in two halves of chymotrypsin separated about the middle of the chain, one folded from the N-terminus toward the C-terminus and the other from the C-terminus toward the N-terminus, forming a symmetrical pattern in the distance map. The results of superposition show that 80% of the internal residues correspond in space. Those results suggest the importance of internal residues for the tertiary structure of a protein.

**Conformational Properties of Poly( $\gamma$ -hydroxy-L-proline) Based on Rigid and Flexible Pyrrolidine Rings.** T. Ooi, D. S. Clark, and W. L. Mattice. *Macromolecules*, **7**, 337 (1974).—Conformational energy maps have been computed for the internal dipeptide unit in poly( $\gamma$ -hydroxy-L-proline) containing planar trans peptide bonds. The conformational energy maps based on rigid pyrrolidine rings which have the conformation observed in the solid state exhibit one low-energy region at  $\psi = 145^\circ \pm 40^\circ$  (using the convention in which  $\phi, \psi = 180^\circ, 180^\circ$  for the fully extended chain). The characteristic ratios for this geometry are much higher than the result obtained experimentally for poly(L-proline). Conformational energy maps based on flexible pyrrolidine rings contain a region of low energy near  $\psi = -50^\circ$  in addition to the low-energy region at  $\psi = 150^\circ \pm 70^\circ$ . The characteristic ratio based on the opportunity for flexibility in the pyrrolidine rings of residues  $i$  and  $i+1$  is close to the result obtained experimentally for poly(L-proline) in water. The configurational entropies per residue for poly(L-proline) and poly( $\gamma$ -hydroxy-L-proline) are  $\sim 3\text{--}5$  cal/(mol deg) smaller than the results obtained by Brant, Miller, and Flory for polyglycine and poly(L-alanine). The hydroxyl group in the  $\gamma$ -hydroxy-L-proline residue decreases the flexibility of the pyrrolidine ring, leading to a smaller configurational entropy for the  $\gamma$ -hydroxy-L-proline residue than for the L-proline residue. This effect would lead to an increased thermal stability of the collagen triple helix when  $\gamma$ -hydroxy-L-proline is substituted for L-proline.